Studies on Growth Mechanism of Murine Sarcoma Cell Line, MS-K

Name ZHONG XiuYing

Doctoral Program in Life and Food Sciences

Graduate School of Science and Technology

Niigata University

Contents	Page No.

Abbreviation	Full Name
VEGF	vascular endothelial growth factor
VEGFR	vascular endothelial growth factor receptor
HIF-1	hypoxia inducible factor-1
TEAD4	transcriptional enhancer factor 1-related protein
shRNA	small hairpin RNA
HS	horse serum
WBC	white blood cell
PLT	platelet
HCT	hematocrit
RBC	red blood cell
H.E.	Hematoxylin and eosin
EGFP	enhanced green fluorescence protein
SATB	special AT-rich DNA binding protein
ESC	embryonic stem cell
TSC	trophoblast stem cell
HSC	hematopoietic stem cell
NSC	neural stem cells
LSC	leukemia stem cell
BM	bone marrow

Abstract

A malignant tumor initiates from a single cell or a small fraction of cells in which the mechanism of cell growth regulation has become modified, leading to change of cell growth potential. Then the successive generations of these cells progressively further advance towards cancer. This progression in different cancer types have been under extensive study. Numbers of genes have been reported to involve in tumor growth, angiogenesis and metastasis. However, the details of these mechanisms have not yet been elucidated. The objective of this study was to elucidate the effect of vascular endothelial growth factor (VEGF-A) on regulation of cell growth and tumor growth of murine sarcoma cell line MS-K tumor.

MS-K-GFP cells were established by transfecting *egfp* gene into MS-K cells. MS-K-GFP cells proliferated rapidly *in vivo*, and died soon after reaching confluence. Inoculation of these cells into mice resulted in tumor formation. While the tumor enters into rapid growth progress, the numbers of red blood cells and platelets, and hematocrit in host mice decreased sharply. It was confirmed that MS-K-GFP tumor did not metastasize to other tissues until day 35 after inoculation by detecting the existence of *egfp* gene by PCR. Well-developed blood vessels were observed in day 35 MS-K-GFP tumor by the paraffin sections. High expression level of *vegf-A* was detected in MS-K-GFP cells.

To elucidate the role of VEGF-A in the formation of non-necrotic MS-K-GFP tumor, stable *vegfA*-knockdown-MS-K-GFP clones (designated as *vegfA*-KD MS-K-GFP) were established using plasmid-based *shRNA* expression vector. Proliferation and colony formation capacity of the *vegfA*-KD MS-K-GFP cells in a semi-solid medium under low serum conditions were significantly lower than that of normal MS-K-GFP cells. In addition, *vegfA*-KD MS-K-GFP cells failed to form tumor while being inoculated into mice. Mice inoculated with *vegfA*-KD MS-K-GFP cells lived without any disorder in peripheral blood cell numbers even until day 50 after inoculation. It was confirmed that *vegf-A* knock down had no effect on expression of *vegf receptor-1* (*vegfr-1*) by quantitative PCR analysis of *vegfr-1*. Since the western blotting of VEGFR-1 revealed the phosphorylation of this receptor, there were no disfunction in this receptor of *vegfA*-KD MS-K-GFP. Furthermore, tumor forming ability of stable *vegfr-1*-knockdown-MS-K-GFP

clones was lower than the control MS-K-GFP. These results suggested that the reduced production of VEGF-A and the impoverished subcutaneous environment lacking growth factors caused the failure of *vegfA*-KD MS-K-GFP tumor formation. Therefore, the VEGF-A produced by MS-K cells, acts as a growth factor for MS-K cell itself by the autocrine signal pathway through VEGFR-1, and supports tumor formation and growth *in vivo* by inducing the blood vessel formation.

Recently, it has been reported that special AT rich sequence binding protein 1 (SATB1), known as a global higher-order chromatin structure organizer and transcription factor, had promoted proliferation and metastasis of cancer cells in various types of cancer. Since the expression of the *satb1* was detected in neither NIH/3T3 nor MS-K, the *satb1* overexpressing NIH/3T3 and MS-K were established. Interestingly, overexpression of the *satb1* induced the expression of the stemness-related gene, *nanog*. Furthermore, the *satb1* overexpressing MS-K cells, designated as *satb1*+ MS-K, are able to form colony even just being cultured in alpha-MEM and formed tumor more rapidly than the control MS-K cells. These data suggested that *satb1* may involve in regulation mechanism of tumor metastasis. The established *satb1*+ MS-K will provide a good model for study on tumor angiogenesis and metastasis.

概要

癌発生の原因は,基本的に細胞の増殖を調節するメカニズムに異常が起こる事にある。数多くの癌関連遺伝子が発見され,これらが腫瘍細胞の増殖，腫瘍血管新生，癌の悪性度に関係することが報告されているが，そのメカニズムについては，まだ充分に判っていない部分が多く残されている。

本研究では，マウス肉腫形成細胞株(MS-K)を用いて，このMS-K細胞の増殖や，この細胞の移植により形成される肉腫の増殖に，血管内皮細胞増殖因子(*vascular endothelial growth factor*-A; VEGF-A) がどのように関与しているかを明らかにした。

まず始めに改良型緑色蛍光タンパク質の遺伝子(*egfp*)を導入したMS-K細胞(MS-K-GFP)を作製した。*In vitro*におけるMS−K−GFP細胞の増殖は速く，細胞密度が高くなるとすぐに死ぬことが分かった。MS-K-GFP細胞を移植して形成される腫瘍が急速に増殖するにつれて，移植したマウスの末梢血中の赤血球数，血小板数およびヘマトクリット値は減少した。*egfp*遺伝子発現を指標としてこの細胞の転移を調べたが，転移は認められなかった。35日目の巨大なMS-K腫瘍組織切片中に壊死はなく，また血管が豊富にあるのが観察された。MS-K腫瘍における豊富な血管新生には血管新生因子が関与していることが考えられたので，RT-PCRにより発現を検討したところ，*vegf-A*, *vegf-C*の発現を検出した。そこで，*RNAi*の手法により*vegf-A*の発現を抑制したMS-K (A-KD)株を樹立した。このMS-K (A-KD)細胞は通常の血清濃度における増殖は正常細胞とほぼ同じであったが，低血清濃度における増殖は正常MS-K−GFP (control)に比べて低く，半固形培地中におけるコロニー形成能も著しく低かった。そしてこの細胞による腫瘍形成を検討したところ，細胞移植後５０日目まで肉腫形成は確認されず，有意にその腫瘍形成能は抑制されていた。なお，マウスの末梢血液細胞数等に変動は認められなかった。この細胞における*vegf receptor-1*の発現は正常MS-K-GFPと比べて，変わらない事が確認された。またWestern blottingにより，そのリン酸化に変化がない事も確認され，このMS-K (A-KD)のVEGF-Receptorが機能的で有る事を示した。MS-K (A-KD)は自身の産生するVEGF-Aの量が少ないということと，皮下という低タンパク質環境下においてその増殖が低いために,マウス皮下に移植しても，十分な肉腫を形成できないものと考えられる。さらにこの*vegf receptor-1*発現をRNAiにより同様に抑制すると，MS−K肉腫の形成が抑制され，MS-Kの増殖にVEGFが重要な役割を持つことを示した。

ところで，最近，多くの遺伝子の発現を調節する転写因子としてSatb1 (Special AT rich sequence binding protein 1)が発見され，癌の悪性化や転移と染色体の立体構造の変化に関係があることが報告されはじめた。MS-Kにおけるこの遺伝子の発現を調べたところ，この遺伝子の発現は検出されなかった。そこで，この遺伝子の役割をさらに解明するために，NIH/3T3細胞においてこの遺伝子を過剰発現させたところ，幹細胞特異的な因子である*nanog*の発現が誘導されることを見いだした。さらにMS-K細胞でもこの遺伝子を過剰発現させ，+satb1-MS-Kを樹立したところ，NIH/3T3と同様に*nanog*遺伝子の発現誘導が確認され

た。さらにこの+satb1-MS-K細胞は通常の培養条件でもコロニーを形成しながら増殖し，マウスに移植するとコントロールに比べて有意に大きい肉腫を形成したため，癌の悪性化に関わっていることが示唆された。

以上の結果より，正常MS-K細胞ではMS-K細胞が産生したVEGF-AはVEGF Receptor-1を通して自己の増殖に働くものと考えられる。また同時に，宿主の細胞に働きかけて血管内皮細胞の増殖を誘導し，その肉腫内部に血管を誘導する事により巨大な肉腫を形成するものと考えられる。また，MS−K細胞での*satb1*の過剰発現の結果から，この遺伝子の制御下に*nanog*遺伝子があり，この幹細胞化に関わる遺伝子の発現はより悪性度の高い癌化を引き起こす可能性が示唆された。今回樹立された*satb1*過剰発現MS-K細胞は，より悪性度の高い癌細胞による血管新生などを研究するのに良いツールを提供するものと考えられる。

Introduction

Blood vessels and lymph vessels are essential for forming a network to supply oxygen, nutrition and signaling molecules to tissue and absorb fluid back to the circulatory system without tissue edema [1, 2]. Under pathological conditions, tumor associated angiogenesis and lymphangiogenesis plays important roles in the rapid growth and metastasis of the tumor tissue [3, 4]. A correlation of VEGF family and tumor angiogenesis and lymphangiogenesis had been documented in a variety of cancer [3-6].

VEGF-A, as a diffusible endothelial cell-specific mitogen and the most potent direct-acting angiogenic protein as known [5-7], has been under extensive study. In different types of cancer, VEGF-A is over-expressed by the carcinoma cells, and facilitates tumor growth and metastasis by stimulating the proliferation and migration of endothelial cells, increasing tumor blood vessel density and accelerating angiogenesis [7, 9]. Recently, the idea of VEGF-A as an autocrine regulator of cell proliferation has been demonstrated in various primary carcinomas [9-13]. VEGF-A and its main signaling receptors, VEGFR-1 or / and VEGFR-2 were found co-expressing in a number of carcinoma cells and activating PI3K or MAPK signaling pathways, which indicates the existence of an autocrine VEGF-A/VEGFR loop in carcinoma cells and lends evidence of the importance of VEGF-A for carcinoma cell survival and proliferation independent of angiogenesis [14]. Therefore, the mechanisms of the regulation activity in tumor formation of VEGF-A are widely accepted as that VEGF-A produced by carcinoma cells, acts in a paracrine fashion on endothelial cells to facilitate angiogenesis in tumor and exerts its effect as an autocrine growth and survival factor on carcinoma cells themselves. With regards to cancer therapy strategies targeting VEGFs and their receptors, some monoclonal antibodies have proven therapeutic benefit. Decoy-soluble receptors and antisense oligonucleotides are also regarded to be potential tools for cancer therapy [15-17]. Recently, RNAi, which is initiated by double-stranded RNA that are homologous to the gene being suppressed, has been demonstrated to significantly degrade mRNA and protein and be more effective in

gene silence than antisense oligonucleotides [15]. Considering no obvious and serious side-effects have been found, VEGF-A siRNA probably could be a new choice of therapy used for clinical trial against cancer [15, 17]. However, in studies involving siRNA, the efficiency, functioning duration and correlation between final results and siRNA induction methods should be further investigated [18].

For over a decade, genes involving in regulation of VEGF-A signal pathway have been under extensive study. It is well-known that hypoxia-inducible factor (HIF)-1α promotes expression of VEGF to stimulate angiogenesis in various kinds of cancer [19]. Transcription of VEGF mRNA is also induced by a variety of growth factors and cytokines, including PDGF, TGF-β1, and IL1-β [20, 21]. Appukuttan B *et al.* documented that the related transcriptional enhancer factor-1 isoform, TEAD(216), appears to inhibit VEGF production independently of HIF, suggesting that TEAD(216) may provide a novel approach to treat VEGF-dependent diseases [22]. A recent study on human ovarian carcinoma showed that the special AT-rich DNA binding protein (*satb1*) was highly expressed in malignant ovarian carcinoma cells and tissues with VEGF-A overexpression, suggesting SATB1 may regulate expression of VEGF-A [23]. SATB1, one of the few global higher-order chromatin structure organizers, involves in gene activation or repression by facilitating assembly of chromatin remodeling proteins and transcription factors and binding of transcription factor complex to active promoter regions of genes [24, 25]. It was well documented to be an important determinant in differentiation of T cells by modulating gene expression in its unique nuclear distribution pattern called ''cage-like'' structure in thymocytes [24, 26]. SATB1 was also reported to effect on the development of brain and epidermis [27-29]. Recent studies revealed that SATB1 and its closely related protein SATB2 act in an antagonistic manner and the relative expression of *satb* proteins involves in keeping the balance of self-renewal and differentiation of embryonic stem (ES) cells by regulating the expression of Nanog [24]. It was also documented that SATB1 protein promoted trophoblast stem (TS) cell renewal and inhibit differentiation in part by regulating the expression of the TS cell stem-associated transcription factor, EOMES [25]. These results suggested that SATB1 plays an

important role in maintaining the state of stem cells. In 2008, Han *et al.* suggested that SATB1 expressed in breast cancer cells promoted tumor growth and metastasis by directly reprogramming the gene expression profile of breast cancer cells [30]. Since then, *satb1* was reported to be expressed in various types of aggressive cancer cells, and contribute to tumor progression [23, 31-34]. SATB1 protein has been proposed as a potential target which could be used to controlling or curing breast cancer in the development of therapeutic strategies [30, 31]. It was also verified that the only small fraction of tumor cells has the ability to initiate a new tumor and this subpopulation of tumor cells possesses the capacity of self-renewal and differentiation similar to normal adult stem cells [35-37]. These cells have been termed cancer stem cells (CSCs). The evidence for the existence of CSCs was first derived from the study of human acute myeloid leukemia (AML) [36, 38]. AML is characterized as a cell autonomous disorder that is initiated by the break of homeostatic state in niche caused by leukemia stem cells (LSCs) [39, 40]. LSCs are one type of CSCs in hematopoietic malignancies [38, 39]. Notably, several CSC characteristics are relevant to metastasis, such as motility, invasiveness and resistance to DNA damage-induced apoptosis [36].

Intrinsic factors such as transcription factors were reported to play critical roles in regulating self-renewal and differentiation of stem cells, which sense the presence of extrinsic growth factors in the environment [40-44]. Nanog, Oct4, Sox2, and Klf4 are known regulators of pluripotency and/or self-renewal, in which Nanog is a homeodomain-containing transcription factor that can sustain pluripotency in ES cells even in the absence of leukemia inhibitory factor (LIF) [24, 45]. These pluripotency genes were also found to have expression in various types of cancer cells and contribute to tumor progression [46, 47].

MS-K was previously established from long-term culture mouse bone marrow stromal cells in our laboratory [48]. However, MS-K cells do not have capability to adhere to hematopoietic stem cells or support their proliferation, comparing to the hematopoiesis supportive stromal cell line MS-5 which shares the same source with MS-K [49]. In contrast, MS-K cells present high expression of *ki-ras* and are able to form a non-necrosis tumor which has fibroblastic appearance and capacity to differentiate into adipocytes at the peripheral region of

tumor while being inoculated to mouse, which made MS-K to be characterized as murine sarcoma cell line.

In present study, it is tried to elucidate the effect of VEGF-A on regulation of growth of MS-K tumor and the roles of *satb1* in cancer progression using MS-K tumor as a model.

Materials and Methods

Cells

MS-K, a sarcoma cell line, was established from a long-term culture of C3H/HeN mouse bone marrow cells by our laboratory [48]. MS-K-GFP was established by transfection of MS-K cells with *pMKit*-neo-*egfp* vector. NIH/3T3 is murine fibroblast cell line, which was originally established from the primary mouse embryonic fibroblast cells [50]. NFSA is a murine fibrosarcoma cell line [51, 52]. F-2, established from an ultraviolet light-induced tumor, is a transformed murine cell line with tumorigenicity and vascular endothelial cell properties [53]. Murine iPS (induced pluripotent stem cells) cell is established by transfection of fibroblast by four transcription factor including, *c-myc, klf4, oct3/4* and *sox2* [54]. These cell lines are maintained in our laboratory according to the original reports. Briefly, MS-K-GFP cells were cultured in alpha-modified minimum essential medium (αMEM) medium supplemented with 10% (vol./vol.) of horse serum (HS), 100 U/mL of penicillin, and 100 μg/mL of streptomycin. NIH/3T3 cells were cultured in Dulbecco's Modified Eagle Medium (D-MEM), supplemented with 5% fetal bovine serum (FBS). The cells were maintained at 37°C in humidified atmosphere of 5% CO_2.

Mice

C3H/HeN mice were purchased from SLC (SLC co. Ltd, Sizuoka, Japan) and bred in specific pathogen-free condition (SPF). Eight to 12 weeks old mice were used in experiment. Animal experiments were performed in compliance with the guidelines of Science Faculty of Niigata University.

Proliferation assay, *in vitro*

Cells were seeded at the density of 4 x 10^4 cells / 35mm dish in culture medium, supplemented with suitable concentration of serum and incubated in the CO_2 incubator at 37°C. Cell suspension was prepared using 0.25% trypsin/PBS after rinse the cells with 0.02% EDTA/PBS twice. Then the number of living cells was counted using 0.4% Trypan blue dye for 3 or 7 days.

Tumor formation assay, *in vivo*

For one cell line, eighteen mice were used. About 1.0 x 10^6 cells were suspended in 0.1 mL of PBS, and then inoculated subcutaneously into mouse. After the inoculation, peripheral blood was taken from vein of eye socket and the number of white blood cells, red blood cells, platelet and hematocrit was counted by auto blood cell analysis apparatus (CELLTAC MED-5180, Japan), respectively. On day 7, 14, 19, 24, 29, and 35, three mice were sacrificed and tumor was excised and the weight was measured.

Paraffin section of tumor tissue

Tumor formed by MS-K-GFP cells inoculation were excised on day 35 post-inoculation, fixed in Bouin's solution over night and rinsed in running tap water. Then tumor was dehydrated in alcohol gradient solution (70%, 90%, 95%, 99% and 100% Et-OH), then in xylene solution for 20 minutes for 3 times. Finally embedded in paraffin. Four μm thick sections were prepared and stained with Hematoxylin and Eosin and observed under microscope.

Preparation of genomic DNA and Assay of tumor metastasis

MS-K-GFP cells inoculated mice were sacrificed on day 35 post-inoculation. Tumor, brain, lung, liver and spleen were excised, and bone marrow cells were prepared from tibia and fibula. The samples were frozen immediately in liquid nitrogen. Then genomic DNA was extracted from each sample by phenol/chloroform method and used as template for analysis the expression of *egfp*.

Analysis of gene expression by RT-PCR

Total RNA from cultured cells or tumor was extracted with Trizol Reagent (Invitrogen, Tokyo, Japan), respectively. DNase-treated (Roche Diagnostics GmbH, Manheim, Germany) total RNA was reverse-transcribed by Transcriptor First Strand cDNA Synthesis Kit (Transcriptor Roche Diagnostics GmbH, Manheim, Germany) to synthesize cDNA. RT-PCR was performed with specific primers using the Master gradient (Eppendorf, Paris, France). *beta-actin* was used as an internal standard. Briefly, the reaction mixture containing *Ex Taq* (TAKARA, Tokyo, Japan), 0.25mM dNTPs, sense and antisense primers (final 0.2 μM, each), diluted cDNA solution (1/10 volume diluted with water) and distilled water was mixed (7 μL). The application program included an initial denaturation at 94°C,

followed denaturation at 94°C, annealing and extension at 72°C. PCR products were cloned into cloning vectors, respectively, and were verified by DNA sequencing. The sequences of primers and annealing temperatures for each gene were summarized in **Table 1**.

Quantification of VEGF-A

Cell condition medium or serum of MS-K-GFP inoculated mice were collected and stocked at -80°C before being used. Mouse VEGF ELISA-based kit (R&D Systems, Inc., MN, USA) was used for quantification of VEGF-A according to the manufacturer' instruction.

Construction of shRNA expression plasmids

siRNA sequence targeting mouse *vegf-A* was designed according to the report of Wang, *et al.* [15], with a nucleotide replacement. The following sense and antisense sequences were used: 5'-AGCCAGCACATAGGAGAGA-3' (sense) and 5'- TCTCTCCTATGTGCTGGCT -3' (antisense). The sequence is located in the forth exon of *Mus musculus vegf-A* (Accession NM001025250), which is transcribed in all the main isoforms of VEGF-A protein. Sense and antisense oligonucleotide containing the sense sequence, 9 bp loop sequence and antisense sequence, with *Bam* HI and *Hind* III restriction sites on the 5' and 3' ends, respectively, were synthesized by FASMAC Co., Ltd. (Kanagawa, Japan). The annealed dsDNA oligonucleotides were inserted into *pSilencer* 4.1-CMV-Hygro (Ambion Inc., Tokyo, Japan) by T4 DNA ligase (TaKaRa, Tokyo, Japan). Then the DH-10 bacteria was transformed and the plasmid DNA was purified. The constructed *shRNA* expression vector was confirmed by double restriction enzymes digestion with *Bam* HI and *Hind* III. The negative *shRNA* control (Scramble) plasmids, with an *shRNA* template sequence having no homologous to genome databases of human or mouse, were supplied by the *pSilencer* 4.1-CMV-Hygro Expression Vector Kit.

Establishment of *shRNA* expression clones

About 1.25 x 10^5 of MS-K-GFP cells were seeded in alpha-MEM supplemented with 10% HS. Transfection was performed after 24 hours with 5 μg of plasmid DNA by using FuGENE HD Transfection Reagent (Roche, Tokyo, Japan) or X-tremeGENE HP DNA Transfection Reagent (Roche, Tokyo, Japan), according to the manufacturer's instructions. Culture medium was replaced by alpha-MEM

supplemented with 10% HS containing Hygromycin B (250 μg/mL) after 48 hours to perform antibiotic selection. Cells were cloned by limiting dilution and maintained in Hygromycin B containing medium. The cells transfected with plasmids of *pSilencer* 4.1-CMV-Hygro-*vegf-A* and *pSilencer* 4.1-CMV-Hygro-scramble were named as the *vegf-A*-KD MS-K and SCR-MS-K, respectively.

Quantitative analysis of gene expression by the real-time PCR

Total RNA from *vegf-A*-KD MS-K, SCR-MS-K and MS-K-GFP cells were extracted with Trizol reagent. One μg of DNase-I-treated RNA was used to synthesize cDNA using the oligo dT12-18 primers in 10μL of reaction volume by Transcriptor First Strand cDNA Synthesis Kit (Transcriptor Roche Diagnostics GmbH, Manheim, Germany). Real-time PCR was performed with gene specific primers and SYBR Premix *Ex Taq* (TaKaRa, Tokyo, Japan) using Light Cycler (Roche Diagnostics GmbH, Manheim, Germany). *Beta-actin* (*β*-actin) was used as an internal standard. Serially diluted plasmid DNA samples were used in each experiment to generate a standard curve. The amplification program included an initial denaturation at 95°C for 30 seconds, followed denaturation at 95°C for 5 seconds, annealing for 20 seconds and extension at 72°C for 15 seconds, for 45 cycles. After PCR, a melting curve program (melting curve method in the Light Cycler software) was completed to confirm the presence of the PCR product in every run. A quantification program (fit point method, also included in the Light Cycler software) was used to determine the amount of initial PCR product in each sample. The level of gene expression was then normalized to the level of *beta-actin* gene expression. For each sample, four reaction mixtures were prepared for each sample, and the PCR reaction was performed at least two times. PCR product was confirmed by electrophoresis. The sequences of primers and annealing temperatures for each gene were summarized in **Table 1**.

Colony formation assay

Cultured cells were harvested and cell suspension was prepared as described above. About 1.0×10^3 cells was suspended in alpha-MEM with 3.2% methylcellulose (final concentration was 0.8%) and various concentration of horse serum (final concentration was 10%, 2% and 0.1%, respectively), then cells were seeded in 35m/m dish. Four parallel experiments for each group were performed. Numbers of colonies were counted on day 11.

Analysis of phosphorylation of VEGFR-1

MS-K (Normal) cells were seeded at the density of 3 x 10^5 cells / 60mm dish in alpha-MEM supplemented with 2% HS. After 2 days, concentration of HS was reduced to 0.2%. After 24 h, the cells were stimulated with 5% HS for 3 or 10 min, respectively. The cell lysate was prepared using RIPA buffer. Approximately 50 μg of the total cell lysate was electrophoresed on 10% SDS polyacrylamide gel and transferred to PVDF membrane. The membrane was treated with anti-Flt-1 antibody (clone Y103; Abcam, Tokyo Japan) at 4°C for 16 h, and then was treated with anti-Rabbit IgG-HRP (KPL, MD, USA) and chemiiluminesence reagent (Immunostar; Wako, Tokyo, Japan). After detecting the signal of VEGFR-1, the membrane was washed with 10% SDS solution to remove the anti-Flt-1 antibody, and then was treated with anti-phosphotyrosine antibody (clone PY20; Biolegend, CA, USA), anti-mouse IgG + IgM-Phosphatase antibody (KPL, Tokyo, Japan) and color development reagent (Bio-Rad, Tokyo, Japan) to detect phosphotyrosine signal. Finally, the membrane was washed again and then was treated with anti-β-Actin antibody (Anaspec Inc. CA, USA) and anti-Rabbit IgG-HRP (KPL) and chemiiluminesence reagent (Immunostar; Wako). The signal was detected by CS analyzer (Atto, Tokyo, Japan).

Analysis of expression of VEGFR-1

Normal MS-K, *vegfA*-KD MS-K, *vegfr-1*-KD MS-K h2, and F2 cells were seeded at the density of 3 x 10^5 cells / 60mm dish in alpha-MEM supplemented with 5% HS. After 4 days, the cell lysate was prepared using RIPA buffer. Approximately 100 μg of the total cell lysate was electrophoresed on 10% SDS polyacrylamide gel and transferred to PVDF membrane. The membrane was treated with anti-Flt-1 antibody (clone Y103; Abcam, Tokyo Japan) at 4°C for 16 h, and then was treated with anti-Rabbit IgG-HRP (KPL, MD, USA) and chemiiluminesence reagent (Immunostar; Wako, Tokyo, Japan). The signal was detected by CS analyzer (Atto, Tokyo, Japan).

Construction of *satb1* expression plasmid

Oligonucleotides were synthesized by BML Co., Ltd. (Tokyo, Japan). The following primers were used to clone Mus musculus *satb1* coding sequence by PCR: 5'- CACCATGGATCATTTGAACGAGGC-3' (sense) and 5'-

TCAGTCTTTCAAGTCGGCATT-3' (antisense). Briefly, the reaction mixture containing PrimeSTAR Max DNA Polymerase (TAKARA, Tokyo, Japan), sense and antisense primers (final 0.2 μM, each), diluted cDNA solution (1/10 volume diluted with water) and distilled water was mixed (50 *μL*). The application program included an initial denaturation at 98°C, followed denaturation at 98°C, annealing at 55°C and extension at 72°C, for 35 cycles. PCR product was cloned into pENTR/SD/D-TOPO Vector (Invitrogen, Tokyo, Japan) and was verified by DNA sequencing. Then the *satb1* insert was cloned into pcDNA6.2/V5-DEST expression vector (Invitrogen, Tokyo, Japan) by Gateway LR Reaction according to the manufacturer' instruction. Sequence of insert was verified by DNA sequencing.

For construction of EF1alpha-*satb1*-IRES-KOrange expression vector, oligonucleotides of *satb1* CDS sense and antisense primers were synthesized by BML Co., Ltd. (Tokyo, Japan). pENTR/SD/D-TOPO-*satb1* plasmid was used as template to amplify *satb1* CDS by PrimeSTAR Max DNA Polymerase (TAKARA, Tokyo, Japan). PCR product was cloned into pMD20-T vector (TAKARA, Tokyo, Japan). After restriction endonuclease digestion and DNA purification, the *satb1* insert was ligation into MCS of EF1alpha-IRES-KOrange expression vector by T4 DNA Ligase (TAKARA, Tokyo, Japan). All of the plasmids was verified by DNA sequencing.

Overexpression of *satb1* in NIH/3T3 cells and MS-K cells

NIH/3T3 cells were cultured in D-MEM, supplemented with 5% FBS and were incubated at 37°C in humidified atmosphere containing 5% CO_2. 1 μg of overexpression vectors were transfected by Xtreme HP Transfection Reagent (Roche Tokyo, Japan) following the manufacturer's instructions (Details were seen in Part 1). For transient overexpression, total RNA of the transfected cells was extracted and gene expression was analyzed. The cells transfected with plasmids of EF1alpha-*satb1*-IRES-KOrange were named as *satb1*+ NIH/3T3 and cells transfected with plasmids of EF1alpha-IRES-KOrange were named as Mock NIH/3T3. For establishment of stably expressing clones, culture medium was replaced by D-MEM medium supplemented with 7.5% FBS containing Blasticidin (8 μg/mL) after 48 hours to perform antibiotic selection. Clones were established

by limiting dilution.

MS-K cells were seeded in alpha-MEM medium supplemented with 5% HS and transfection was performed after 24 hours with 1 μg of plasmid DNA by using X-tremeGENE HP DNA Transfection Reagent (Roche, Tokyo, Japan) following the manufacturer's instructions. Culture medium was replaced by alpha-MEM medium supplemented with 5% HS containing Blasticidin (10 μg/mL) after 48 hours to perform antibiotic selection. Cells were maintained in Blasticidin containing medium. The cells transfected with plasmids of pcDNA6.2/V5-DEST-*satb1* or pcDNA6.2/V5-DEST mock vector were named as *satb1*+ MS-K and mock MS-K, respectively.

Statistical Analysis

All results present as means ± SD. For statistical analysis, one-way ANOVAS and multiple comparison tests (Tukey-Kramer's honestly significant difference (HSD) test) were performed using the JMP software (SAS Institute Japan, Tokyo, Japan), and statistical significance was set at $p<0.05$ (presented as *) or $p<0.01$ (presented as **).

Table 1. Primers for RT-PCR and quantitative RT-PCR

Gene	Accession No.	Forward sequence (5'-) Reverse sequence (5'-)	Product Size (bp)	Annealing Temp. (°C)
vegf-A	NM001025250	gaccctggctttactgctgta	303	58.0
		gtgaggtttgatccgcatgat		
vegf-C	NM009506	aacgtgtccaagaaatcagcc	388	61.0
		agtcctctcccgcagtaatcc		
vegfr-1	NM010228	tgaggagctttcaccgaact	130	59.1
		tatcttcatggaggccttgg		
vegfr-2	NM010612	ggcggtggtgacagtatctt	162	60.5
		gtcactgacagaggcgatga		
vegfr-3	NM00829	gacaagcactgccacaagaa	194	61.8
		aggtcgattcccgactcttt		
beta-actin	NM007393	cagggtgtgatggtgggaatggg	408	64.0
		caggatggcgtgagggagagca		
egfp	GU564446	atggtgagcaaggg	720	60.0
		ttacttgtacagctcgtc		
satb1	NM_001163630.1	gcagaacgggagccctctaggaaga	696	62.0
		tggttggcaccttgctggga		
satb2	NM_139146.2	ggaggtttgatgattccagtt	281	57.4
		acgtgatagacatcttgcagc		
satb1(for qPCR)	NM_001163630.1	gatcatttgaacgaggcaact	174	56.5
		gtgttttaaaggcactccctg		
p53	NM_011640	aacttaccagggcaactatg	232	58.0
		gtgggggcagcgtctcac		
p21	NM_007669	gtcttgcactctggtgtctga	112	58.0
		gcgcttggagtgatagaaatc		
cdk2	NM_183417.3	acctagtgtgtacccagcacc	282	58.0
		acttggggaaacttggcttat		
cdk4	NM_009870.3	acaagtaatgggaccgtcaag	288	58.0
		tagagatacctctcgaggcca		
p27	BC014296.1	gtgagagtgtctaacgggagc	123	58.0
		agtcccgggttagttcttcat		
beta-catenin	NM_001165902.1	catctgtgctcttcgtcatct	339	58.0
		gagagctccagtacacccttc		
nanog	NM_028016.2	agggtctgctactgagatgctctg	365	62.0
		caaccactggtttttctgccaccg		
oct4	NM_001252452.1	ggcgttctctttggaaaggtgttc	313	62.0
		ctcgaaccacatccttctct		
sox2	NM_011443.3	tagagctagactccgggcga	293	62.0
		ttgccttaaacaagaccacgaaa		
klf4	NM_010637.3	gcgaactcacacaggcgagaaacc	709	62.0
		tcgcttcctcttcctccgacaca		
endoglin	NM_007932.2	caatgccagcattgtcacctcc	428	68.0
		agaggctgtccatgtcgatgca		

Sequences of PCR primers, predicted product sizes and annealing temperatures were listed. All the PCR products were cloned and confirmed by DNA sequencing.

Results

MS-K-GFP has rapid growth *in vitro*

MS-K cell line was established in our laboratory by Shirata *et al.* from murine long-term bone marrow culture [48]. MS-K-GFP, *egfp* gene transfected MS-K, was established in order to use EGFP as a marker of this cells for analysis of tumor metastasis *in vivo*, or distinguish this cells in co-culture with other cells, *in vitro*.

The cell growth curve of MS-K-GFP was shown in **Figure 1**. Comparing to NIH/3T3, MS-K-GFP proliferated rapidly, proliferation peak appeared on day 4, and then they died soon after reaching confluence. Cytomorphological observation showed that most of the cells adhered to the bottom of culture dish in 24 hours after incubation, and got the confluence more than 80% on day 4. The cells began to detach from the culture dish soon after reaching confluence and almost no adherent cells could be seen after 7 days.

MS-K-GFP forms non-necrosis tumor rich in blood vessels without metastasis *in vivo*

MS-K-GFP was injected subcutaneously with 1.0 x 10^6 of cells per mouse into 15 mice. Tumor was excised on day 7, 14, 19, 24, 29, and 35. As shown in **Figure 2A**, tumor grew slowly in the early days post-inoculation, and then it entered into a rapid growth phase from day 19. No necrosis was observed in excited MS-K-GFP tumor (**Figure 2B-G**). Tumor on day 35 post-inoculation was excised and HE-stained sections were prepared. The presence of the well-developed blood vessels in MS-K-GFP tumor may contribute to non-necrotic tumor formation (**Figure 2H**).

Genomic DNA of tumor, brain, lung, liver, spleen and bone marrow of MS-K-GFP cells inoculated mice on day 35 after inoculation were used as PCR templates. Results of PCR using the *egfp* specific primers suggested that MS-K-GFP tumor did not metastasize to other tissues until day 35 post-inoculation (**Figure 2I**).

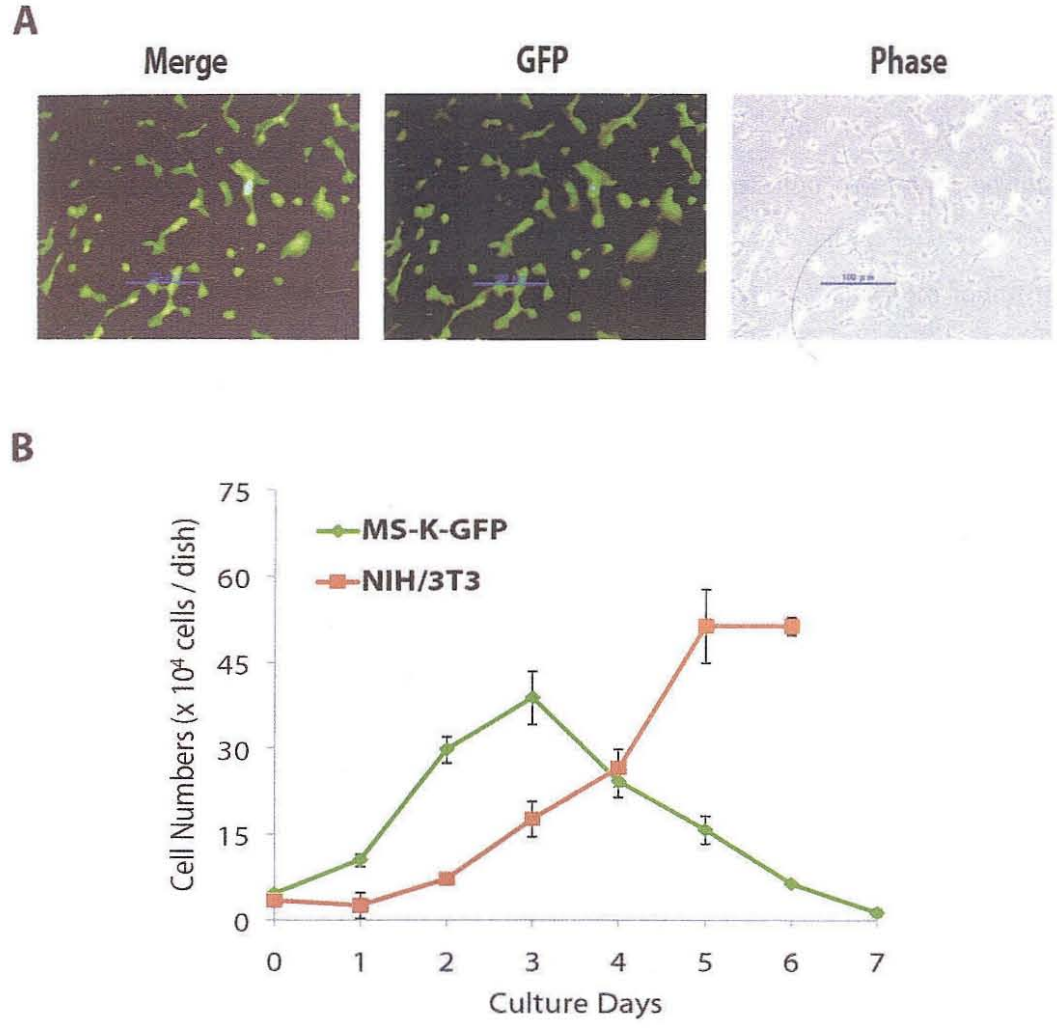

Figure 1. Growth curve of MS-K-GFP

A. MS-K-GFP showed green fluorescence. **B**. Growth curve of MS-K-GFP. MS-K-GFP or NIH/3T3 cells were seeded at the density of 4 x 10^4 cells / 35mm dish in culture medium, respectively. Number of living cells was counted for 6 or 7 days. Data presents mean ± S. E.

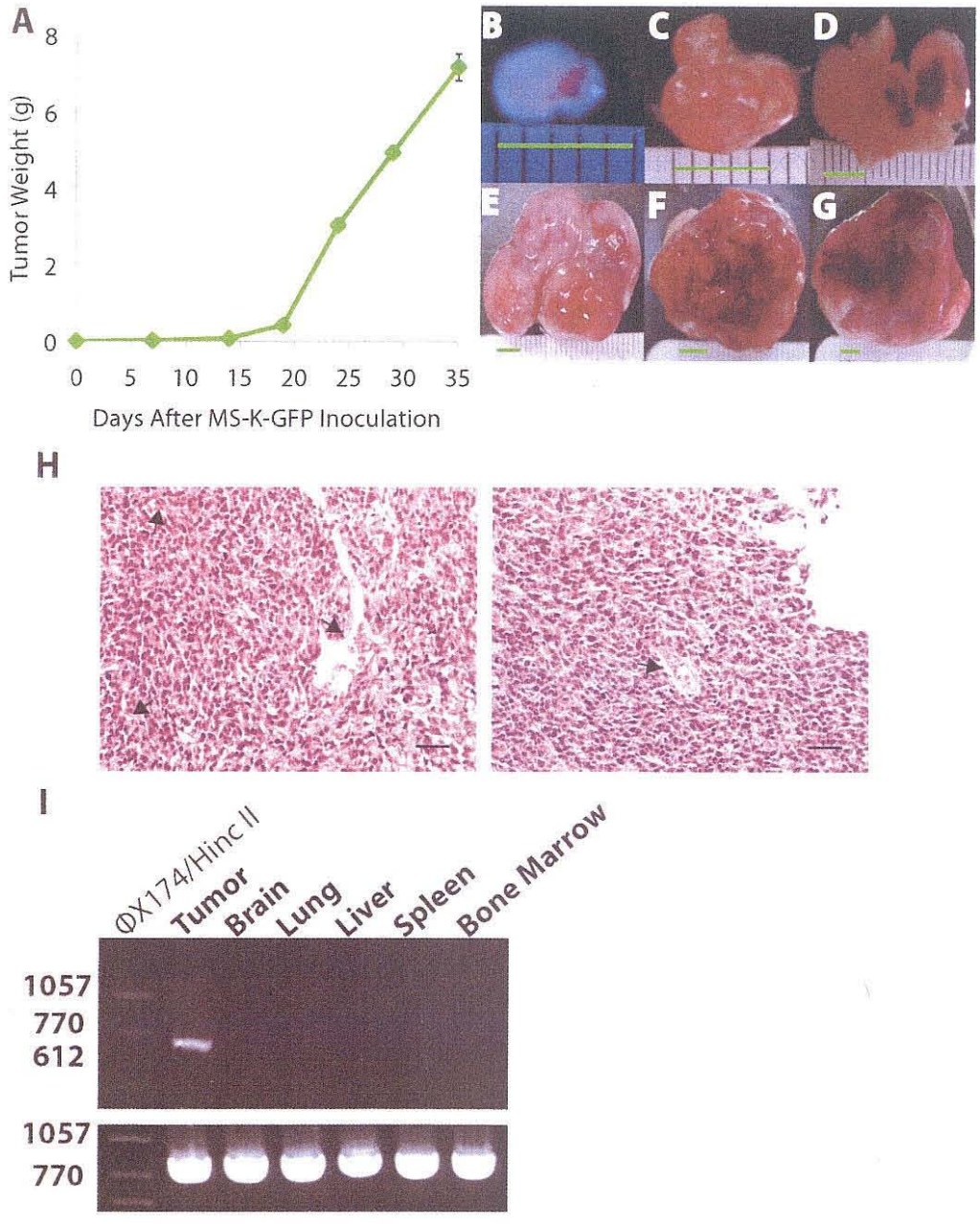

Figure 2. Tumor formation by MS-K-GFP

A. Growth curve of MS-K-GFP-tumor. About 1 x 10^6 MS-K-GFP cells were inoculated subcutaneously into each mouse. Tumors were excised and weighed to make tumor growth curve. Data presents mean ± S. E. **B - G**. MS-K-GFP tumor on day 7, 14, 19, 24, 29 and 35, respectively (Scale Bar: 5 mm). **H**. Blood vessels in MS-K tumor. Day 35 MS-K-GFP tumor was excised from mouse and paraffin-embedded sections were stained with H.E. (Bar: 20 μm). Arrowheads show the blood vessels. **I.** No metastasis in MS-K tumor. Genomic DNA was extracted from several tissues to check the metastasis of MS-K-GFP tumor by *egfp* PCR.

Hematological feature of MS-K-GFP-inoculated mice

As shown in **Figure 3**, the number of white blood cell (WBC) decreased sharply on day 7 post-inoculation and followed a sharp increase. Then it increased mildly, and reached 3 times more than that of the control ones on day 35. The numbers of red blood cell (RBC) and platelet (PLT) and percentage of hematocrit (HCT) seemed normal until day 19, presented a sharp decrease on day 19, and then kept at low level. These data supported that tumor cells had an absolute requirement for a persistent supply of nutrition from blood to nourish for their rapid growth, or the tumor would become necrotic or apoptotic.

The *vegf-A* has augmented expression during tumor growth

Expression profiles of *vegf-A*, *vegf-C*, and their receptor *vegfr-1*, *vegfr-2*, and *vegfr-3* at day 14 and at day 35 MS-K-GFP tumor were detected by RT-PCR (**Figure 4**). Day 35 tumor showed to have augmented expression levels of *vegf-A* and its receptor *vegfr-1*. Although no difference in expression level of *vegf-C* was detected, expression of its receptor *vegfr-3* was increased in day 35 tumor.

Serum from MS-K-GFP inoculated mice was collected on day 0, 14, 18 and 28 post-inoculation. ELISA based quantification assay of VEGF-A in the mice serum confirmed that the level of VEGF-A was increasing during tumor growth process, and then it kept in a high level with no more increase on day 28 (**Table 2**). Considering tumor growth curve together, the data suggested that MS-K-GFP tumor growth was corresponding to quantification of VEGF-A in serum.

MS-K-GFP is strong positive of *vegf-A*

Expression of *vegf-A* and its receptors in MS-K-GFP and other cell lines was analyzed by RT-PCR (**Figure 5**). Both *vegf-A* and *vegfr-1* were expressed in MS-K-GFP cells, while the expression of its other receptor, *vegfr-2*, was not detected. MS-K-GFP cells expressed high level of *vegf-C*, but not *vegfr-3*, the receptor of *vegf-C*. Endothelia cell line F2 expressed the *vegf-A* and the three receptors, but not *vegf-C*. Murine fibrosarcoma cell line, NFSA, and fibroblastic

cell line NIH/3T3 expressed *vegf-A*, *vegf-C*, and only *vegfr-1*.

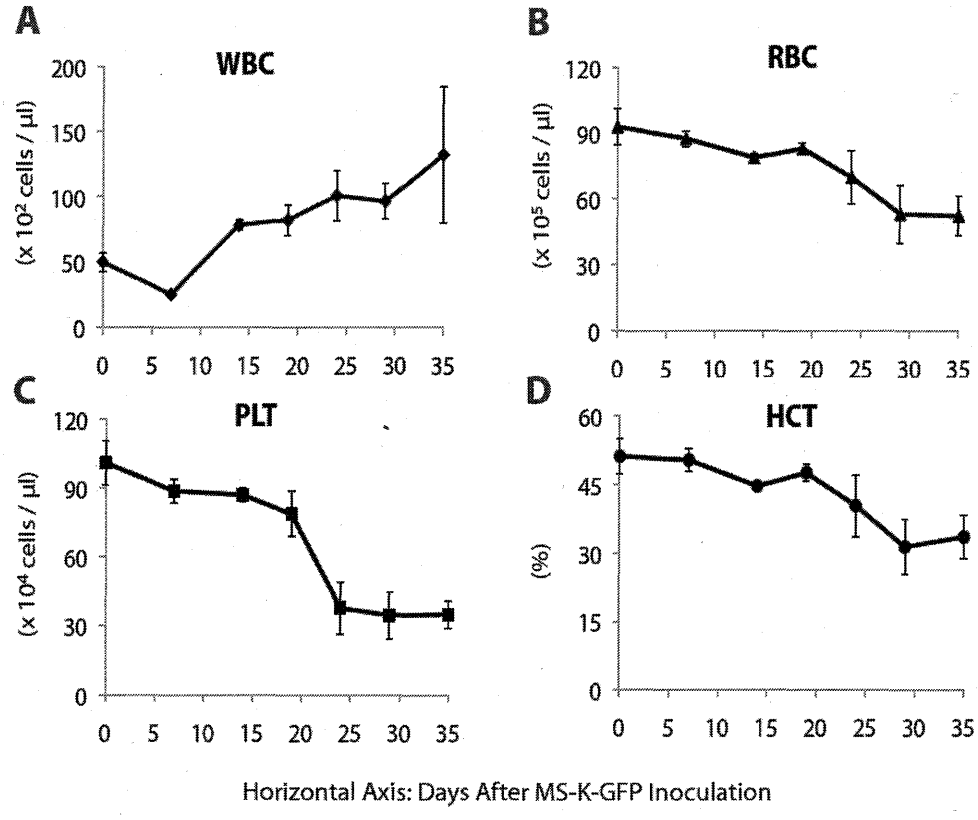

Figure 3. Hematological features of MS-K-GFP inoculated mice

Peripheral blood assay of MS-K-GFP inoculated mice was performed periodically. Peripheral blood was taken from vein of eye socket and numbers of white blood cells (**A**), red blood cells (**B**), and platelets (**C**) were counted and percentage of hematocrit (**D**) was measured. Data represents mean ± S. E.

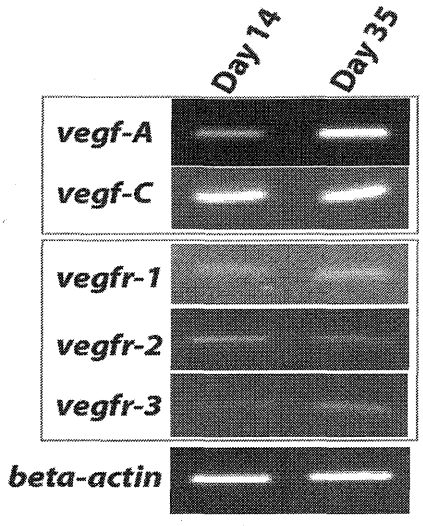

Figure 4. Expression profiles of *vegf* family in MS-K-GFP tumor

cDNA was prepared from day 14 or day 35 tumor, respectively. Expression of *vegf-A*, *vegf-C*, and their receptors *vegfr-1*, *vegfr-2*, and *vegfr-3* was analyzed by RT-PCR.

Table 2. Quantification of VEGF-A in Serum of MS-K-GFP inoculated mice

Days after MS-K inoculation	Conc. of VEGF-A in serum (pg/mL)
0	157.0 ± 20.0
10	232.1 ± 68.1
14	296.5 ± 131.5
18	574.7 ± 45.6
28	450.5 ± 17.9

Serum samples were prepared from MS-K-GFP inoculated mice on day 0, 10, 14, 18, 28 after inoculation, respectively. Quantification of VEGF-A in serum was assayed by Mouse VEGF ELISA-based kit. Data represents mean ± S. E.

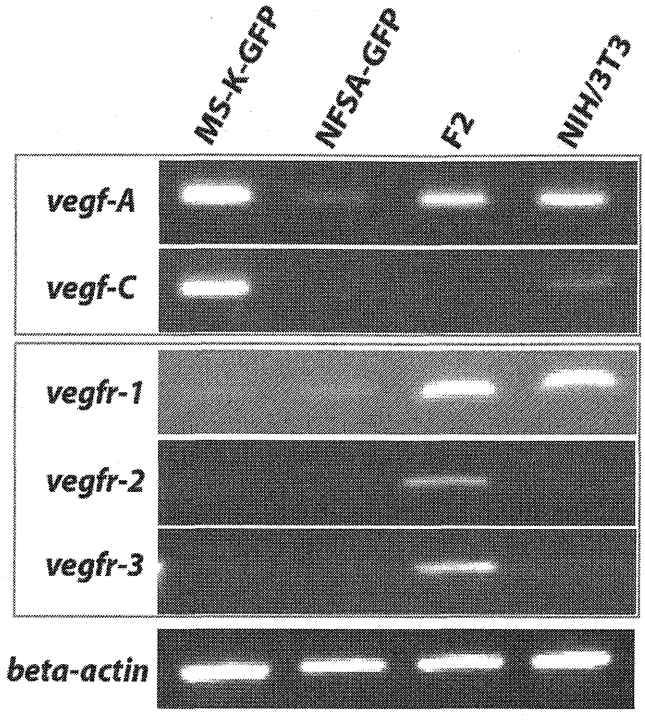

Figure 5. Expression Profiles of *vegf* family in MS-K-GFP and other cell lines

cDNA was prepared from MS-K-GFP, NFSA-GFP, F2 and NIH/3T3 cells, respectively. Expression of *vegf-A*, *vegf-C*, and their receptors *vegfr-1*, *vegfr-2*, and *vegfr-3* was analyzed by RT-PCR.

Expression level of *vegf-A* in MS-K-GFP was significantly suppressed by plasmid-based knock down vector

Targeting sequence of *the vegf-A* was designed in the forth exon of mouse *vegf-A* gene. All the main isoforms of VEGF-A share this exon. The *vegf-A*-target *shRNA* expression vector was induced into MS-K-GFP cells. After antibiotic selection, 4 of HygromycinB-resistant clones were established, and expression level of the *vegf-A* was analyzed by quantitative PCR (qPCR) (**Figure 6**). The expression levels of *vegf-A* were significantly suppressed in clone 3 (20.5% of the level in SCR MS-K-GFP) and clone 2 (27.5%), and expression in clone 1 and clone 4 was 81.6% and 91.3% of that in control cells (SCR MS-K-GFP), respectively. In subsequent experiments, clone 3 (named as *vegfA*-KD MS-K-GFP) was used, because of its highest knock-down efficiency.

In order to confirm the knock down efficiency, culture condition medium of normal MS-K-GFP, SCR MS-K-GFP and *vegfA*-KD MS-K-GFP was collected and the levels of VEGF-A was quantified by ELISA (**Table 3**). As expected, production of VEGF-A in *vegfA*-KD MS-K-GFP was approximately half of that in normal MS-K-GFP under low serum culture condition. The results indicated that plasmid-based knock down efficiently suppressed expression of *vegf-A* in *vegfA*-KD MS-K-GFP cells. The significant difference between negative control and normal MS-K-GFP may be caused by the damage of proteins while the sample was stocked before being used.

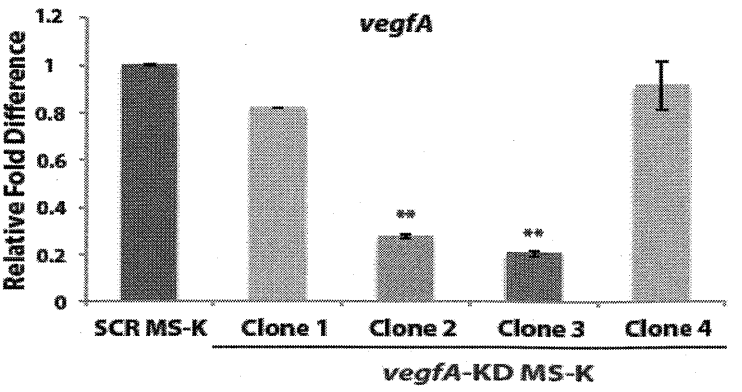

Figure 6. Establishment of the *vegf-A* knock down MS-K-GFP clones

Short hairpin RNA interference (*shRNAi*) vector for *vegf-A* was constructed and transfected into MS-K-GFP cells. After Hygromycin B selection, four clones were established by limiting dilution method. cDNA was prepared from each clone and expression level of *vegf-A* and *beta-actin* was analyzed by quantitative PCR (qPCR). Then the relative expression of *vegf-A* against *beta-actin* was calculated. Expression of the control (MS-K-SCR) was set to 1. Data represents mean ± S. E. Asterisks means significant difference ($p < 0.01$).

Table 3. Quantification of VEGF-A in cell condition medium

Cells	Quantification of VEGF-A (pg/mL)	
	Concentration of HS in medium (%)	
	0.1	2
Normal MS-K	444.8 ± 11.6	893.2 ± 8.9
SCR MS-K	241.2 ± 13.6 *	879.2 ± 0.3
vegfA-KD MS-K	217.3 ± 88.2 *	894.7 ± 11.3
Without cells	ND	15.2 ± 7.6

Normal MS-K, SCR-MS-K and *vegfA*-KD MS-K cells were cultured in alpha-MEM supplemented with 0.1% or 2.0% horse serum (HS) at a density of 5 x 10^4 cells / well in 24-well plate. Quantification of VEGF-A was assayed by ELISA kit. Data represents mean ± S. E. Asterisks means significant difference ($p < 0.05$).

The *vegfA*-KD MS-K-GFP cells failed to form tumor, *in vivo*

It was confirmed that MS-K-GFP cells were able to form non-necrotic tumor with well-developed blood vessel system *in vivo* (**Figure 2**). In order to investigate the roles of VEGF-A in tumorigenesis and angiogenesis, the *vegfA*-KD MS-K-GFP, SCR MS-K-GFP and normal MS-K-GFP cells were inoculated subcutaneously into C3H/HeN mice (15 mice in each group).

Interestingly, the *vegfA*-KD MS-K-GFP cells failed to form tumor *in vivo* (**Figure 7A**), in contrast, both normal MS-K-GFP and SCR MS-K-GFP formed tumors. Mice inoculated with *vegfA*-KD MS-K-GFP cells lived without any obvious disorders even on day 50 after inoculation. This experiment was performed twice and only 1 of the 33 *vegfA*-KD MS-K-GFP inoculated mice was found to form a tumor with delayed growth compare to the MS-K-GFP tumor and SCR MS-K-GFP tumor. Growth curve of the cells indicated that there was no difference between the growth of *vegfA*-KD MS-K-GFP and that of MS-K-GFP or SCR MS-K-GFP cells while being cultured under 10% serum condition (**Figure 7B**), suggesting a possibility that the growth of *vegfA*-KD MS-K-GFP could be rescued by some factors in the serum.

The hematological features of *vegfA*-KD MS-K-GFP inoculated mice also presented to be normal without any change, which gave a supportive evidence to that no disorder happened in *vegfA*-KD MS-K-GFP inoculated mice. In contrast, the hematological features of SCR MS-K-GFP inoculated mice changed in a similar pattern as that of nomal MS-K-GFP inoculated ones (**Figure 7C-F**).

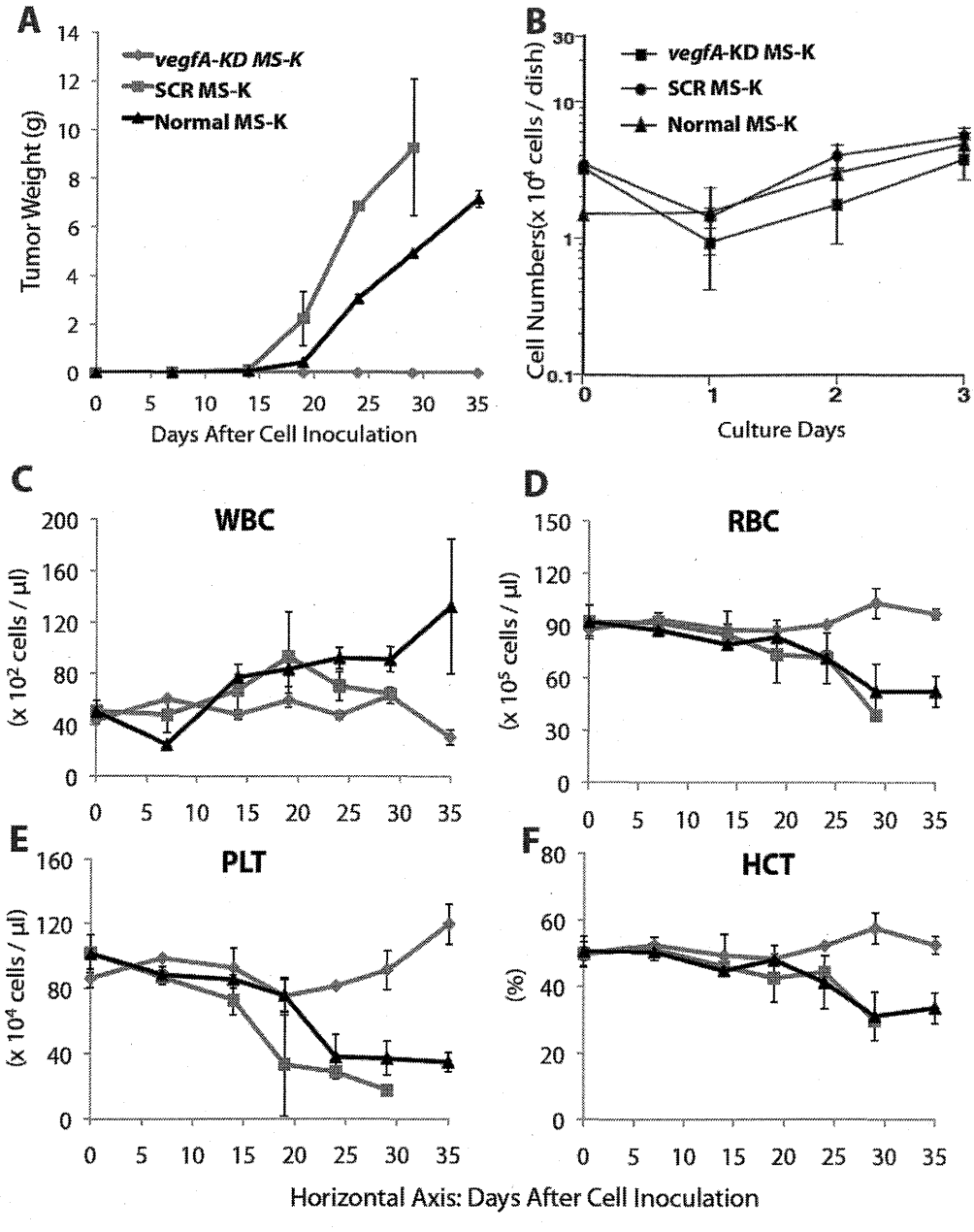

Figure 7. Effect of *vegf-A* knock down on MS-K-GFP tumor formation

A. About 1 x 10^6 of *vegfA*-KD MS-K-GFP, SCR-MS-K-GFP and normal MS-K-GFP cells were inoculated subcutaneously into mouse (1x10^6 cells per mouse and 15 mice in each group). Tumor was excised and weighed to make tumor growth curve.

B. The *vegfA*-KD MS-K-GFP, SCR-MS-K-GFP and normal MS-K-GFP cells were seeded at the density of 4 x 10^4 cells / 35mm dish with 10% HS, respectively. Number of cells was counted with 0.4% Trypan blue staining for 3 days. **C-F**. Peripheral blood assay was performed periodically. Data represents mean ± S. E.

Growth and colony-forming efficiency of *vegfA*-KD MS-K-GFP cells were suppressed in low serum concentration culture condition

In order to confirm whether the growth of the *vegfA*-KD MS-K-GFP was rescued by the factors in the serum, proliferation of *vegfA*-KD MS-K-GFP cells were cultured in medium with different serum concentration. As expected, a significant slow cell growth of *vegfA*-KD MS-K-GFP was observed when the concentration of serum supplemented was reduced to 0.1% (**Figure 8A**). Colony-forming efficiency of *vegfA*-KD MS-K-GFP was assayed in a semi-solid medium supplemented with serum concentrations of 10%, 2%, and 0.1% (**Figure 8B**). Consistent with the cell growth, *vegfA*-KD MS-K-GFP had significantly lower colony-forming efficiency than normal MS-K-GFP and SCR MS-K-GFP cells in low serum concentration culture condition.

Existence of VEGF-A was detected in horse serum (**Table 2**) suggesting that VEGF-A supplied by serum made up the quantification of VEGF-A necessary for MS-K-GFP growth. Therefore, results suggested that the suppression of *vegf-A* expression restrained the proliferation of *vegfA*-KD MS-K-GFP and VEGF-A supplied by serum rescued the cell growth.

VEGF-A-dependent MS-K proliferation signaling

The expression of *vegfr-1* in *vegfA*-KD MS-K-GFP, SCR MS-K and normal MS-K was examined by qPCR and no difference was detected (**Figure 9**), which meant the suppression of *vegf-A* expression in *vegfA*-KD MS-K-GFP did not influence expression level of *vegfr-1*. Considering the co-expression of *vegf-A* and *vegfr-1* in MS-K-GFP, it is hypothesized that VEGF-A / VEGFR-1 autocrine loop signaling regulated survival and growth of MS-K-GFP cells.

In order to confirm the activation of VEGFR-1 in MS-K-GFP cells, phosphorylation of VEGFR-1 was analyzed by western blotting (**Figure 10**). Normal MS-K-GFP cells were cultured in low HS concentration condition, and stimulated with 5% HS for 3 or 10 min, respectively. The results showed that VEGFR-1 in MS-K-GFP cells was phosphorylated and functionally active for signal transduction. There were no difference detected in expression or

phosphorylation of VEGFR-1 between starved MS-K-GFP cells and the HS-stimulated ones, indicating that quantification of VEGF-A produced by MS-K itself was enough to fit the require of activating the phosphorylation of VEGFR-1. Therefore, HS stimulation did not change the expression and phosphorylation of VEGFR-1 in MS-K-GFP cells.

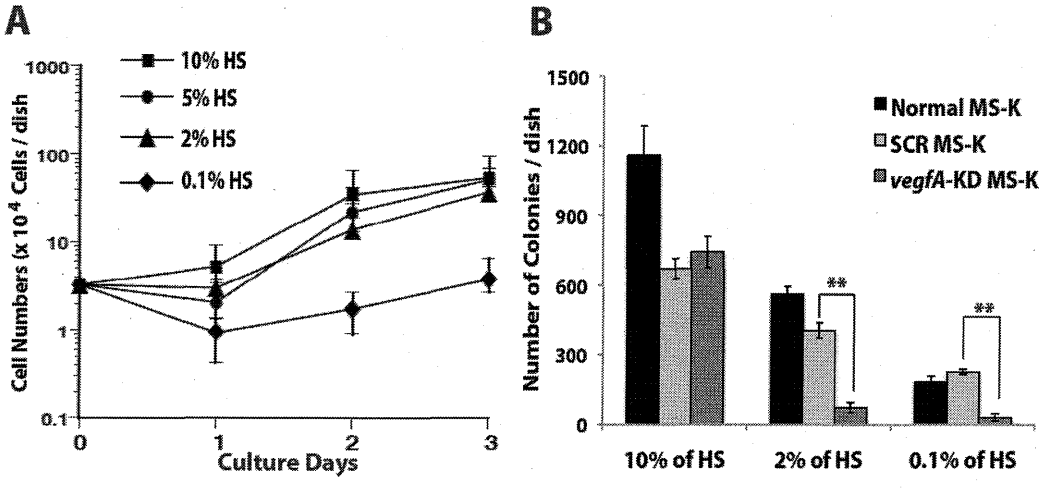

Figure 8. Growth and colony forming efficiency of *vegfA*-KD MS-K-GFP

A. *vegfA*-KD MS-K-GFP cells were seeded at the density of 4 x 10^4 cells / 35mm dish in alpha-MEM supplemented with HS at the concentration of 10%, 5%, 2% and 0.1%, respectively. Living cells number was counted for 3 days. **B**. About 1 x 10^3 cells of normal MS-K-GFP, SCR MS-K-GFP or *vegf-A*-KD MS-K-GFP cells were seed in mixture of alpha-MEM and 0.8% methylcellulose supplemented with HS concentrations of 10%, 2% and 0.1%, respectively. Number of colonies was counted on day 11. Data represents mean ± S. E. Asterisks means significant difference ($p < 0.01$).

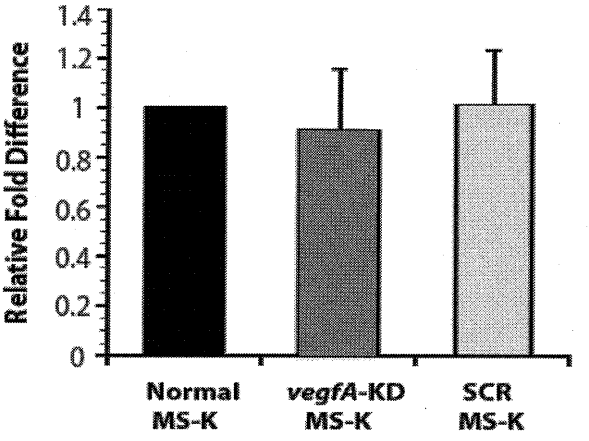

Figure 9. Expression of *vegf receptor-1* in *vegfA* KD MS-K-GFP

Expression of the *vegf receptor-1* was quantitatively analyzed by qPCR using the cDNA prepared from MS-K-GFP, *vegfA*-KD MS-K-GFP, and SCR-MS-K-GFP cells. Data presents relative expression of the *vegfr-1* against the *beta-actin*. Data represents mean ± S. E.

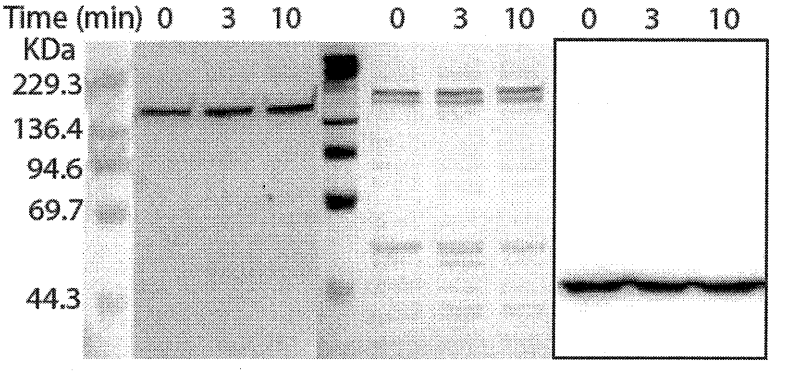

Figure 10. Western Blotting of Phosphorylation of VEGFR-1

Starved MS-K (Normal) cells were stimulated with 5% HS for 3 or 10 min, respectively. Total cell lysate was electrophoresed on 10% SDS-polyacrylamide gel and transferred to PVDF membrane. Expression of the VEGFR-1 was detected by anti-FLT-1 antibody, and phosphorylation of the VEGFR-1 was detected by anti-phosphotyrosine antibody. Expression of β-Actin was also detected in the same membrane as a loading control. Anti-FLT-1 is the left one, anti-phosphotyrosine is in the middle, and anti-β-Actin is the right one.

Down-regulation of VEGFR-1 in MS-K-GFP also suppressed growth of MS-K-GFP tumor

The *vegf-A*-target *shRNA* expression vectors with Hygromycin B or Puromycin resistant gene was induced into MS-K-GFP cells. After antibiotic selection, 4 clones were established, and expression levels of *vegfr-1* was analyzed by qPCR (**Figure 11AB**). The expression levels of *vegfr-1* were significantly suppressed in clone p3 of Puromycin resistant ones (45.6% of the level in Normal MS-K-GFP) and clone h1 (16.9%), h2 (1.8%), h3 (9.6%) and h4 (2.9%) in HygromycinB resistant group.

The knock down efficiency was confirmed by western blotting using anti-FLT1 antibody (**Figure 11 C**). VEGFR-1 in clone h2 of *vegfr1*-KD MS-K-GFP was significantly reduced, comparing to that in normal MS-K-GFP, SCR MS-K-GFP, *vegfA*-KD MS-K-GFP. Clone p3 and h2 of *vegfr1*-KD MS-K-GFP cells were injected into mice. As expected, it was observed that no tumor formed in Clone h2 injected mice and in clone p3 inoculated mice, tumor growth was delayed compare to that in normal MS-K-GFP inoculated ones (**Figure 12**). This results lent evidence to that VEGF-A/VEGFR-1 signal promotes formation and growth of MS-K-GFP tumor.

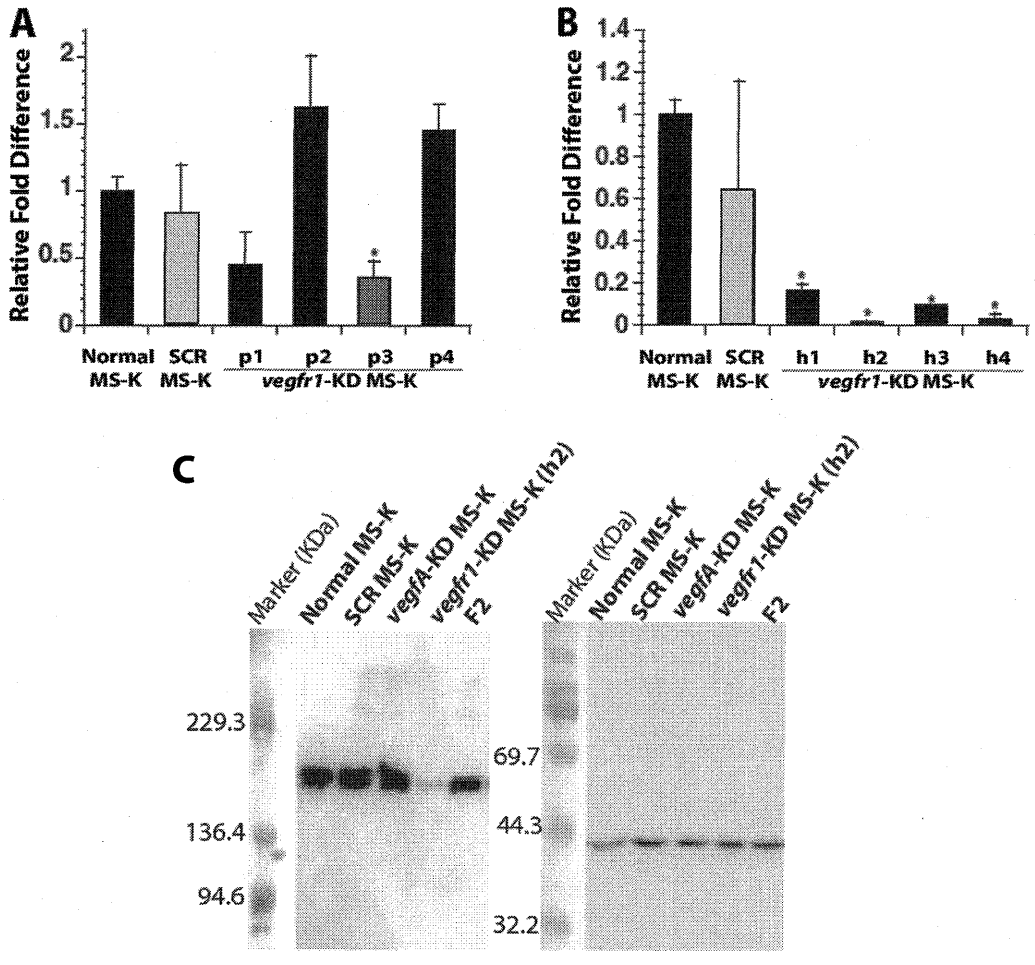

Figure 11. Establishment of the *vegfr-1* Knock down MS-K-GFP clones

A&B. *Short hairpin RNA* interference (*shRNAi)* vectors for *vegfr-1* were constructed and transfected into MS-K-GFP cells. After Puromycin or Hygromycin B selection, four clones for each were established by limiting dilution method. cDNA was prepared from each clone and expression level of *vegfr-1* and *beta-actin* was analyzed by quantitative RT-PCR. Then the relative expression of *vegfr-1* against *beta-actin* was calculated. Expression of normal was set to 1. Data represents mean ± S. E. Asterisks means significant difference. **C.** Quantification of VEGFR-1 was analyzed by western blotting using anti-Flt-1 antibody. β-Actin was used as loading control. Anti-Flt-1 is the left one, and anti-β-Actin is the right one.

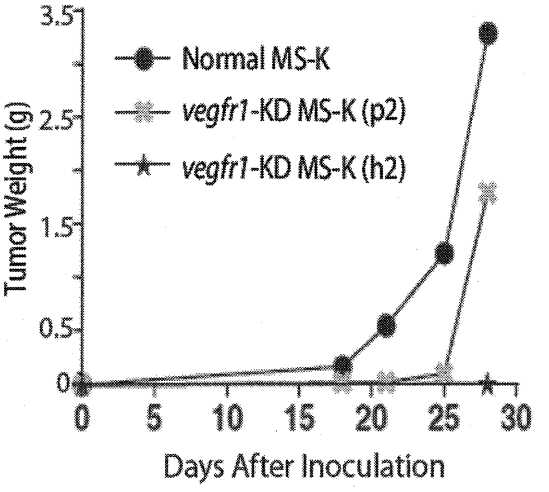

Figure 12. Effect of *vegfr-1* knock down on MS-K-GFP tumor formation

About 1 x 10^6 of *vegfr1*-KD MS-K-GFP (Clone p2 or h2) and normal MS-K-GFP cells were injected subcutaneously into mouse ($1x10^6$ cells per mouse and 15 mice in each group). Tumor was excised and weighed to make tumor growth curve.

The *satb1* had general expression in most tissues in adult mouse *in vivo*

Total RNA from adult mouse liver, intestine, heart, lung, kidney, thymus, and brain was extracted, respectively, and expression of *satb1* and its closely related protein *satb2* was analyzed by RT-PCR (**Figure 13**). Most tissues were detected to have positive expression of *satb1*, although it was weak except that in thymus. In contrast, *satb2* was only expressed in intestine and kidney. Expression of *satb1* and *satb2* in cell lines was also analyzed by RT-PCR (**Figure 14**). Expression of *satb1* was detected in iPS cells and the culture mixture of ES cells and feeder cell SNL cells, but not in fibroblast cell line NIH/3T3, SNL, or hematopoietic supportive stromal cell line MS-5. *satb2* was expressed not only in stem cells, but also in the differentiated cells. Interestingly, in all the murine tissues and cell cultures examined here, in *satb1* positively expressing samples, *satb2* had no expression or weaker expression, while those, which had no expression of *satb1*, highly expressed *satb2*, suggesting the antagonistic expression patterns of *satb1* and *satb2*. Considering these data together, it was supposed whether *satb1* was expressed just in the small population of primary cells, like stem cells or progenitor cells in these tissues.

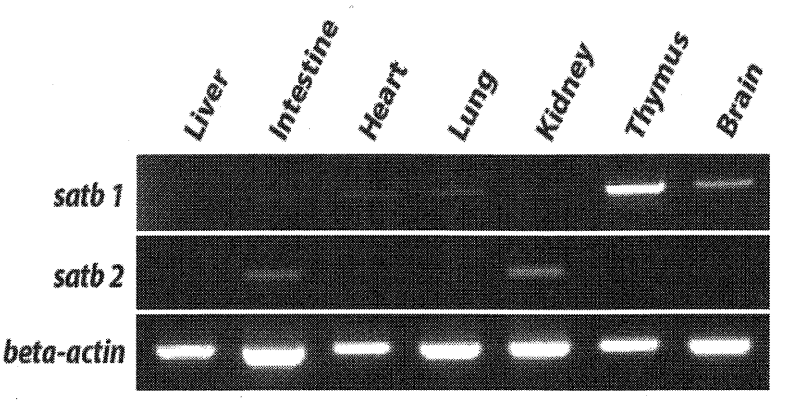

Figure 13. Expression of *satb1* and *satb2* in murine tissues

Expression of *satb1* and *satb2* in various tissues was analyzed by RT-PCR.

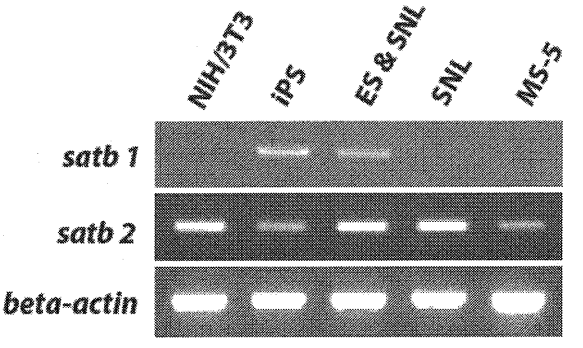

Figure 14. Expression of *satb1* and *satb2* in iPS cells and ES cells

Expression of *satb1* and *satb2* in NIH/3T3 (fibroblast cell line), iPS cells (induced pluripotent stem cells), culture mixture of ES cells (embryonic stem cells) and SNL (iPS feeder cell line), SNL, and MS-5 (hematopoiesis supportive stromal cell line) was analyzed by RT-PCR.

Transient expression of *satb1* in NIH/3T3 cells induced expression of *nanog*

To investigate the potential role of *satb1* in self-renewal and differentiation of stem cells or cell reprogramming, EF1alpha-*satb1*-IRES-KOrange expression vector was transfected into NIH/3T3 cells (**Figure 15A**). The expression of *satb1*, and stemness marker *nanog* and *klf4* was confirmed by RT-PCR (**Figure 15B**). Interestingly, expression of *nanog* was induced by overexpression of *satb1*, whereas the expression of *klf4* was not altered.

Stably *satb1* overexpressing NIH/3T3 cells displayed down-regulated expression of *satb2*

To confirm the result in transient expression, 2 clones of *satb1* stably overexpressing NIH/3T3 cells were established by transfecting pcDNA6.2/V5-DEST-*satb1* into the cells (**Figure 16A**). The *satb2* was found to be down-regulated in *satb1* overexpressing cells, which was consistent with the results observed in previous analysis (**Figure 13, 14**).

Up-regulated expression of *p21* and down-regulated expression of *cdk2* were observed in *satb*1 overexpressing NIH/3T3 Cells

To analyze the activity of *satb*1 in cell cycle, transcription levels of genes related to apoptosis, cell cycle, and *wnt* signal were analyzed by qPCR (**Figure 17B**). All of the genes analyzed here had significantly alterative expression levels in Clone 1, but rarely of them was changed in Clone 4 except *bcl-2* and *cdk2*. Expression of *bcl-2*, which involving in anti-apoptosis and differentiation, was suppressed in Clone 1 but enhanced in Clone 4. Up-regulated expression of *p21* and down-regulated expression of *cdk2* were observed in both of the *satb*1 overexpressing NIH/3T3 cells, although the alternation of *p21* was not significantly different, which may be caused by the increased standard deviation. The *p21*, also known as cyclin-dependent kinase inhibitor 1, binds to and inhibits the activity of cyclin-CDK2, and thus functions as a regulator of cell cycle progression at G1 phase. The suppressed growth of both clones of *satb*1

overexpressing NIH/3T3 cells in partially confirmed the arrest of cells at G1 phase (**Figure 17A**).

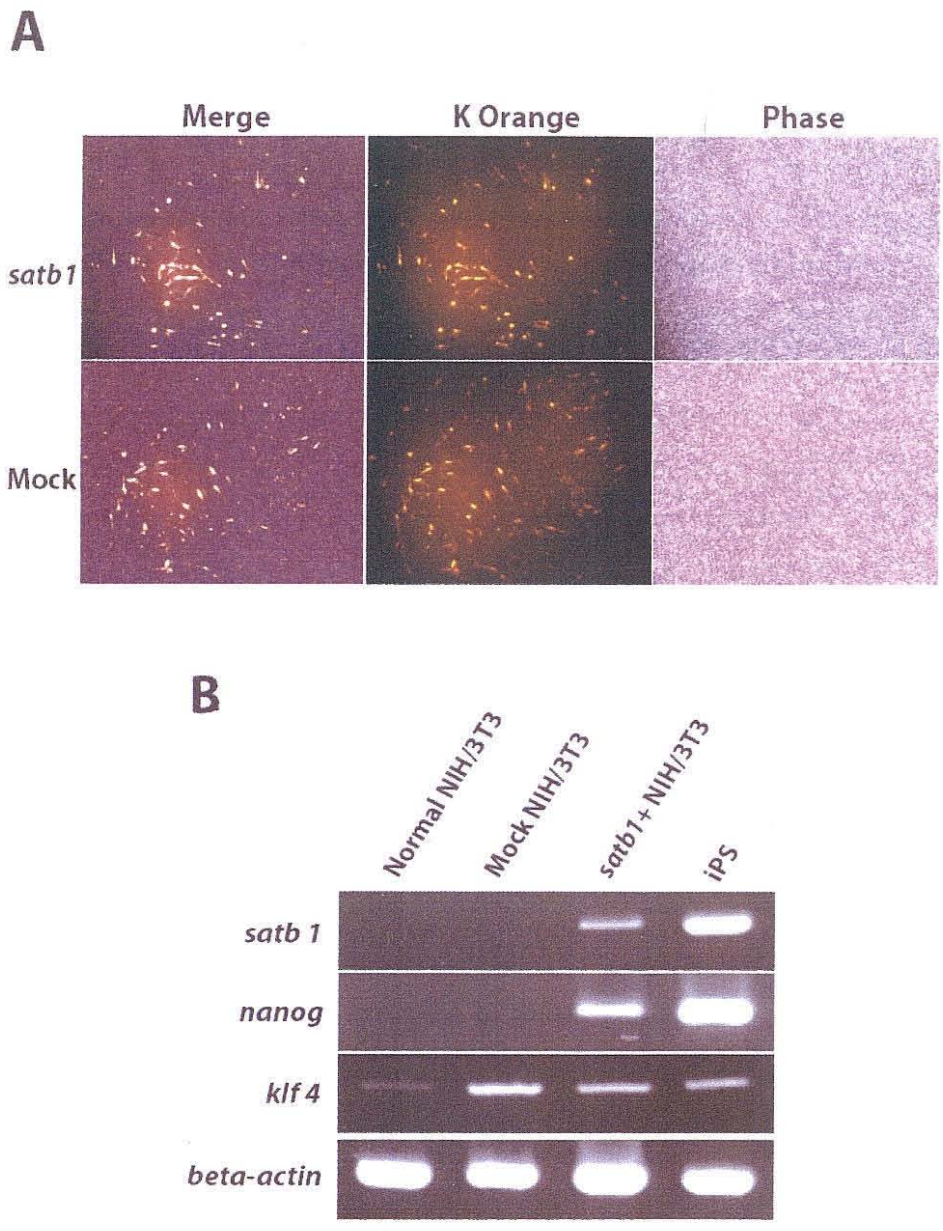

Figure 15. Transient overexpression of *satb1* in NIH/3T3

A. *EF1alpha-satb1-IRES-KOrange* vector was constructed, then NIH/3T3 was transfected. After 3 days, transient expression of Kusabira Orange (KOrange) was detected by fluorescent microscope. Upper low shows the NIH/3T3 cells transfected by *EF1alpha-satb1-IRES-KOrange* and under low show the NIH/3T3 cells transfected by the *EF1alpha-IRES-KOrange* vector (Mock vector). **B.** Expression of *satb1, nanog* and *klf4* was analyzed by RT-PCR.

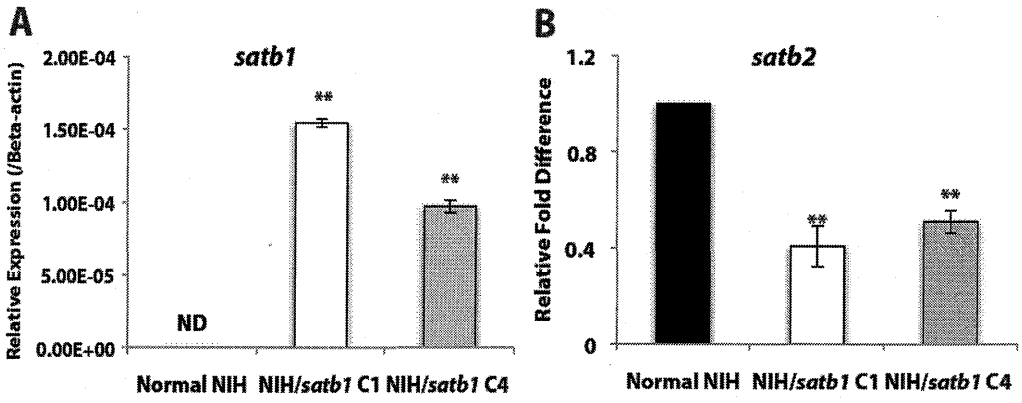

Figure 16. Establishment of *satb1* overexpressing NIH/3T3 clones

NIH/3T3 cells were transfected with *pcDNA6.4-satb1-blasticidin vector*, then antibiotics selection was carried out. Clone C1 and clone C4 were established. Expression of the *satb1*, *satb2* and *beta-actin* in these cell lines was analyzed by qPCR. Then the relative expression of the *satb1* and *satb2* against *beta-actin* was calculated. Data represents mean ± S. E. Asterisks means significant difference ($p < 0.01$).

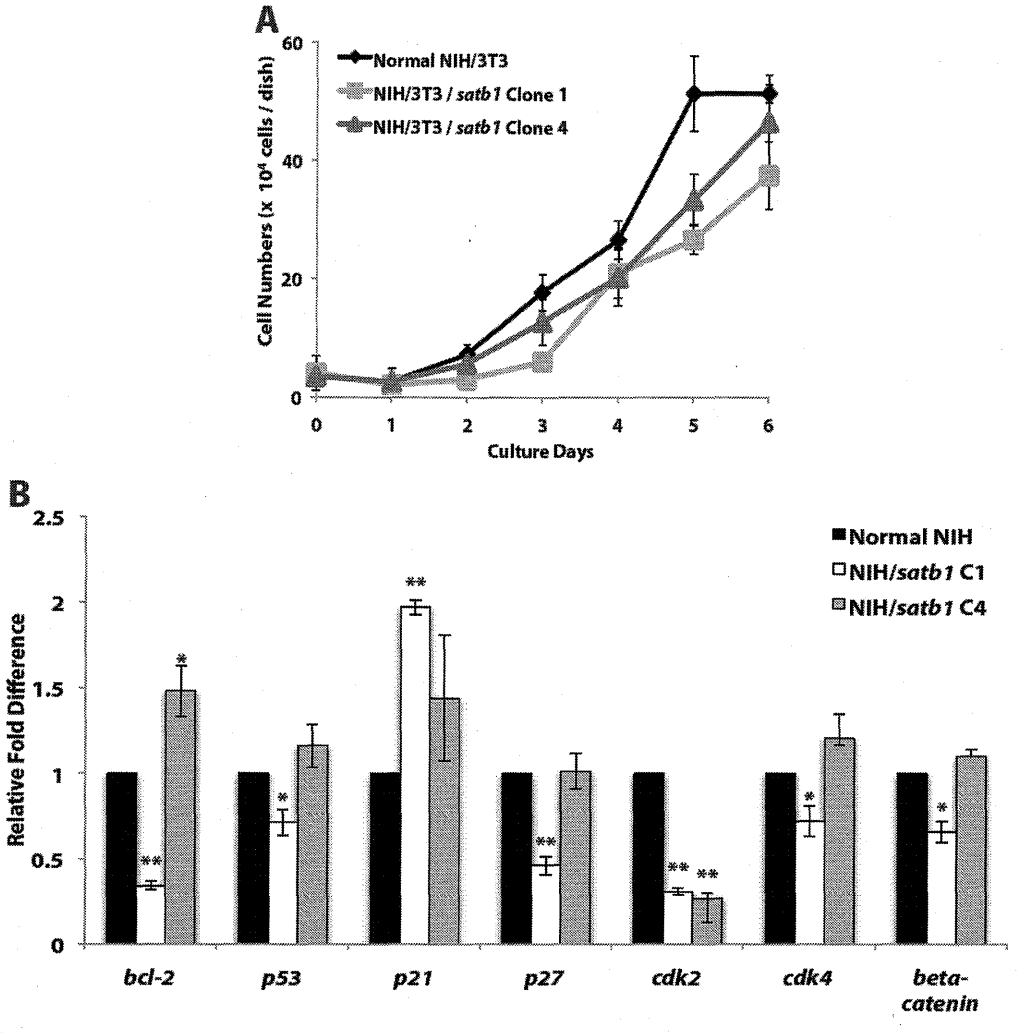

Figure 17. Growth and gene expression of *satb1* overexpressing NIH/3T3 cells

A. Control NIH/3T3 cells, the *satb1* overexpressing NIH/3T3(clone 1 and clone 4) were seeded at the density of 4 x 10^4 cells, respectively. Number of cells was counted. **B.** Expression of genes, related to apoptosis or cell cycle was analyzed by qPCR. Data represents mean ± S. E. Asterisks means significant difference (*, $p < 0.05$; **, $p < 0.01$).

Induced expression of *nanog* was also observed in *satb1* stably expressing clones

As expected, induced expression of nanog was also observed in *satb1* stably overexpressing NIH/3T3 cells and the expression level of *nanog* was dependent to that of *satb1* (**Figure 18A**). Regretfully, expression of other stemness markers, *oct4* and *sox2*, was not detected and there was no difference in *klf4* expression between *satb1* overexpressing NIH/3T3 cells and normal NIH/3T3 cells (**Figure 18B**). These data suggested that *satb1* might involve in cell reprogramming, but not the definitive one.

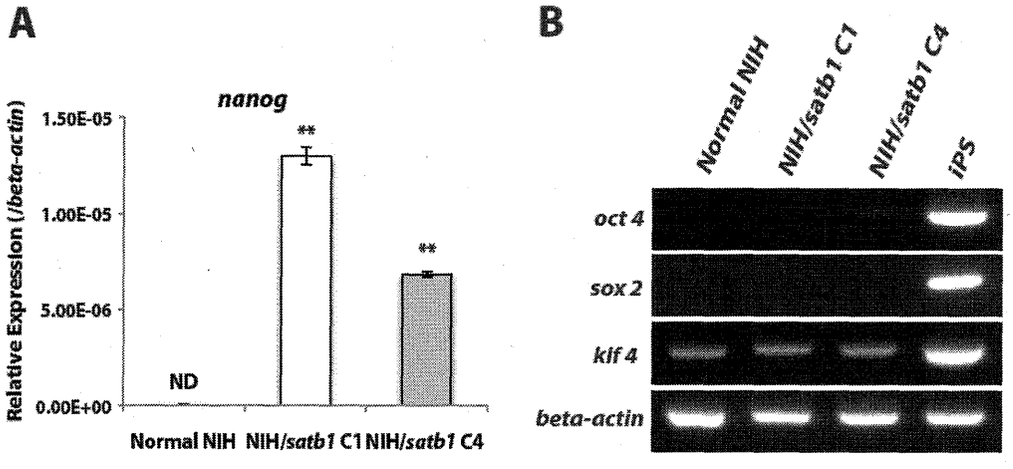

Figure 18. Induction of expression of *nanog* by *satb1* in NIH/3T3

A. Expression of the *nanog* was quantitatively analyzed. Clone 1 and clone 4 of *satb1* overexpressing NIH/3T3 were significantly higher than the normal NIH/3T3. Data represents mean ± S. E. Asterisks means significant difference ($p < 0.01$). **B.** Expression of *oct 4, sox2* and *klf4* was not detected in the clone C1 and the C4. iPS is the induced pluripotent stem cells.

Overexpression of *satb1* has no effect on expression of *vegf-A* in MS-K

MS-K tumor has been regarded as non-metastatic tumor (**Figure 2I**). To see whether the non-metastatic character of MS-K relates to SATB1, expression of *satb1* and its related protein *satb2* in cultured MS-K cells and day 35 MS-K tumor was analyzed by RT-PCR. The result showed that MS-K has no expression of *satb1* (**Figure 19A**), which may be one of reasons caused no metastasis of MS-K tumor.

In order to investigate the role of *satb1* in tumorigenesis the relationship between VEGF-A and SATB1 using MS-K tumor as a model and, MS-K overexpressing *satb1* gene was established (named as *satb1*+ MS-K) (**Figure 19B**). MS-K transfected with mock vector was named as Mock MS-K. Unexpectedly, no difference in expression of *vegf-A* in *satb1*+ MS-K and normal MS-K or Mock MS-K was detected.

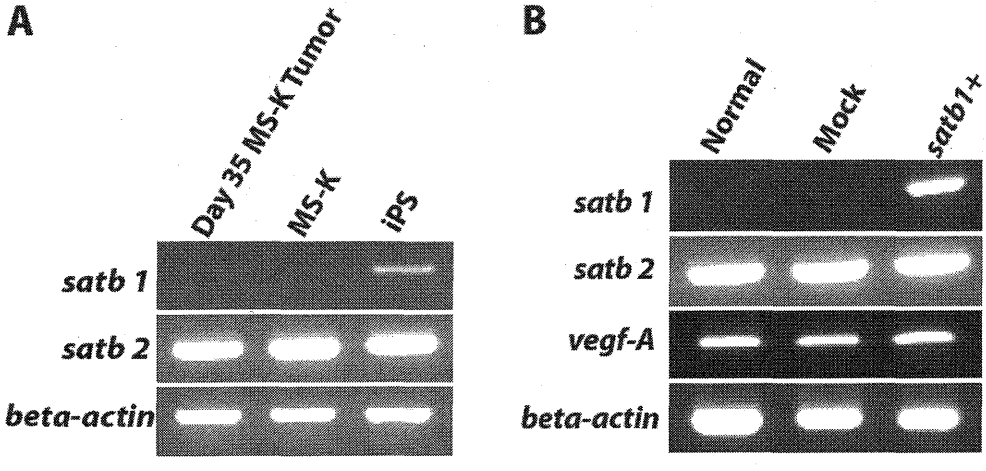

Figure 19. Overexpression of *satb1* in MS-K cells

A. Expression of *satb1* and its related protein *satb2* in day 35 MS-K tumor and MS-K cells was analyzed by RT-PCR. **B**. An expression vector for the *satb1* was constructed and transfected into MS-K cells (designated as *satb1*+ MS-K). Mock vector was also transfected into MS-K cells (designated as Mock MS-K). Expression of the *satb1, satb2, vegf-A* and *beta-actin* was analyzed by RT-PCR.

Expression of *nanog* was also induced in *satb1* overexpressing MS-K cells, and *cdk 2* and *bcl 2* are up-regulated in MS-K cells

A qPCR analysis was performed to monitor expression of genes regulating cell cycle and apoptosis and stem cell marker genes in *satb1* overexpressing MS-K cells (**Figure 20**). Consistent with that in NIH/3T3 cells, induced expression of *nanog* was also observed in *satb1* overexpressed MS-K cells. In contrast to the reduced expression of *endoglin* in Mock MS-K cells, expression of *endoglin* in *satb1* overexpressed MS-K cells showed to be increased. Also, the expression of *cdk2*, known as one of the cell cycle progression promoting factors, and *bcl2* was found to be up-regulated. The up-regulated expression of these stemness genes, anti-apoptosis gene and cell cycle promoting gene was expected to endue MS-K some new features.

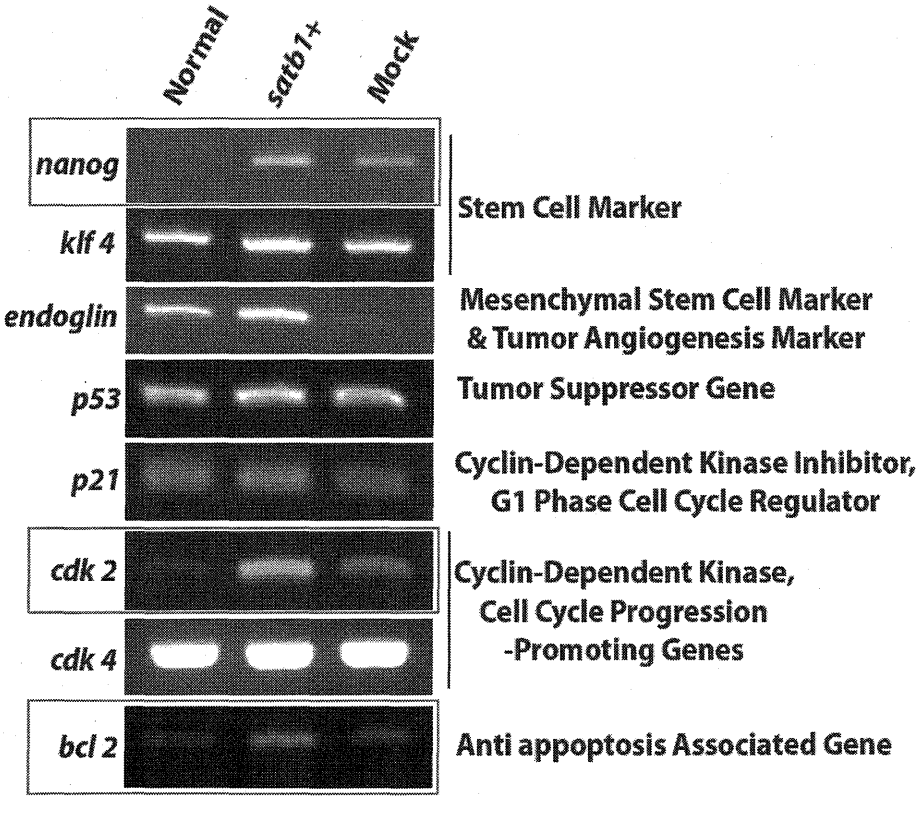

Figure 20. Expression profiles of genes in the *satb1* overexpressing MS-K

Expression of stem cell markers and genes related to cell cycle and apoptosis in the *satb1* overexpressing MS-K cells was analyzed by RT-PCR.

The *satb1* overexpressed MS-K has enhanced colony formation ability

The *satb1*+ MS-K cells were observed to form colony even just being cultured in alpha-MEM medium (**Figure 21A**), which suggested overexpression of *satb1* improved the colony formation ability of MS-K cells. In contrast, both normal MS-K and Mock MS-K exhibit anchorage dependent growth, and will die soon after reaching confluence (**Figure 21A**). No difference in cell growth was observed between *satb1*+ MS-K and normal MS-K or Mock MS-K. However, growth curve showed that *satb1*+ MS-K kept living for short time instead of dying soon after reaching confluence, which was significantly different from normal MS-K and Mock MS-K. The increased expression of *bcl2* may contribute to new character of MS-K cells.

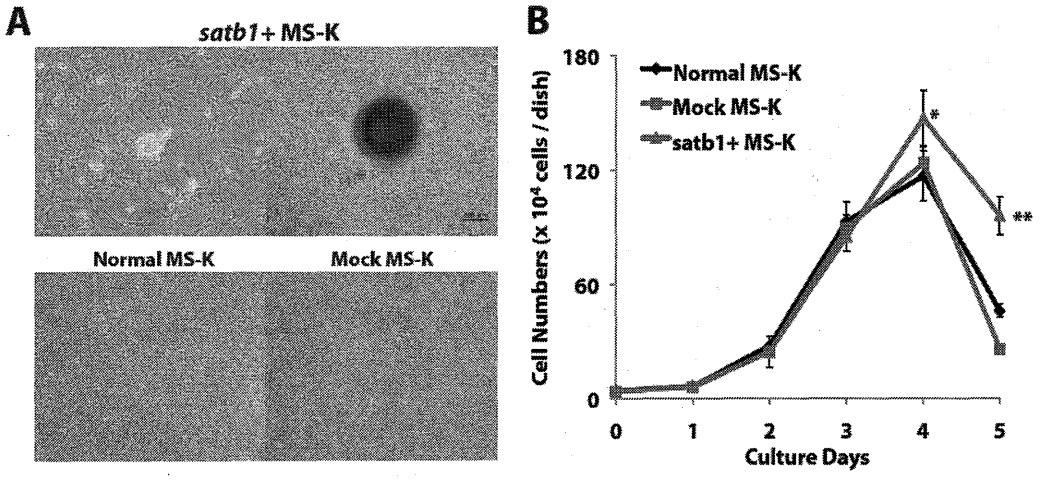

Figure 21. Growth of *satb1*+ MS-K cells, *in vitro*

A. Upper row photographs show the colony formation of the *satb1*+ MS-K (left is 2 and right is day 4). Lower left and right photographs shows the normal MS-K and the mock MS-K at day 4, respectively. **B**. The *satb1*+ MS-K cells, the normal MS-K cells and the mock MS-K cells were seeded in culture dish, respectively. Number of living cells was counted using Trypan blue dye. Data represents mean ± S. E. Asterisks means significant difference (*, $p < 0.05$; **, $p < 0.01$).

The *satb1*+ MS-K tumor grow faster than normal MS-K tumor

The *satb1*+ MS-K cells and normal MS-K cells were injected into mice (15 mice in *satb1*+ Group and 5 in Normal Group). As shown in **Figure 22**, visible tumor could be seen in 57% *satb1*+MS-K inoculated mice just on day 4 after inoculation and tumor formation was confirmed in 93% of *satb1*+ MS-K inoculated mice on day 7, while most Normal MS-K inoculated mice were observed to form visible tumor since day 7 after inoculation.

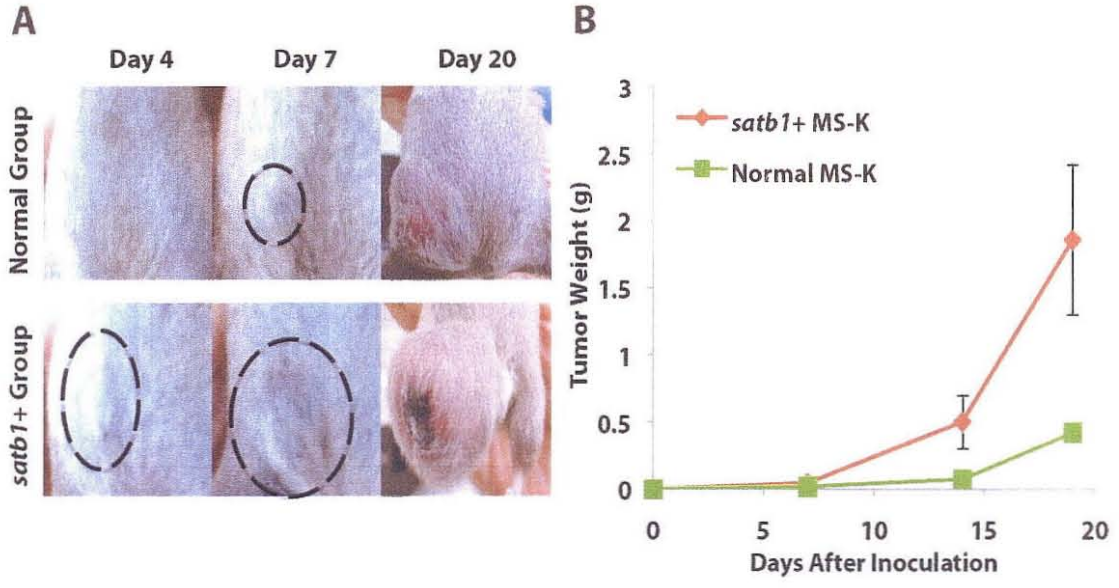

Figure 22. Tumor formation in *satb1*+ MS-K-inoculated mice

Five mice were inoculated normal MS-K, and 14 mice were inoculated the *satb1*+ MS-K cells (1x 10^6 cells/mouse). **A.** Upper row shows the tumor of normal MS-K inoculated mice at day 4, 7 and 20. Under row shows the tumor of the *satb1*-inoculated mice at day 4, 7, and 20, respectively. **B.** Growth of the *satb1*-overexpressing MS-K tumor *in vivo*. Data presents mean ± S. E.

Discussion

Angiogenesis is the sprouting of new blood vessels from the pre-existing ones, which initiates from the induction of the destruction of the pre-existing blood vessels and acceleration of proliferation of endothelial cells. Then myocytes grow surrounding the tubular structure assembled by endothelial cells to form vessels [2, 3]. Although the *in vitro* induction of the capillary from EB body was reported to be successful [10], the mechanisms of blood vessels formation are still far from elucidation. In the other hand, it is well-known that there is angiogenesis spout in variety of tumor tissue to supplement of oxygen and nutrients for the tumor rapid growth, otherwise, the tumor cannot exceed 2-3mm^3 in the hypoxia condition and tumor cells will undergo necrosis [2]. Therefore, growing tumor is also regarded to be a good model for angiogenesis study. MS-K used in present study is a murine sarcoma cell line, which is able to form non-necrotic tumor with well-developed blood vessel system (**Figure 2**).

The mechanisms of switching angiogenesis on in the tumor growth progress involve quite a number of cytokines and regulators, and the key signaling system is VEGFs and their cognate receptors [3]. The crucial step of angiogenesis is the proliferation and migration of endothelial cells for neovascularation. VEGF-A has been shown to play an important role in proliferation, survival, sprouting and migration of endothelial cells and vascular permeability [8, 18]. Therefore, in order to elucidate the effects of VEGF-A on angiogenesis in MS-K tumor progress, *vegf-A* knock down MS-K cells were established. It was well reported that the down-regulation of expression of VEGF-A in various carcinoma cells caused the delay of tumor growth, the inhibition of adhesion of tumor cells to the extracellular matrix and the decrease of tube formation in tumor tissue [16].

However, in our work, inhibition of VEGF-A expression in MS-K cells completely suppressed tumorigenesis. When the expression level of *vegf-A* decreased to 20.5% of that in the control cells (**Figure 6**), *vegfA*-knock down MS-K cells were unable to form tumor in the inoculated mice even after 50 days post-inoculation (**Figure 7A**). Furthermore, hematological features of *vegfA*-knock down MS-K cell-inoculated mice were showed to be normal (**Figure 7C-F**). It

was revealed that *vegfA*-knock down MS-K cells underwent necrosis before the formation of phanerous tumor. The results suggested that the cell necrosis might be partly caused by the failure of inducing blood vessels from host mice to support tumor growth, but mostly by loss of VEGF-A, an important self-survival regulator involved in MS-K cell growth. The autocrine VEGF-A signaling had been found in variety of carcinoma cells, including melanoma cells, leukemia cells, prostate carcinoma cells, colon carcinoma cells, bladder tumor and breast carcinoma cells [4-8, 11, 12]. Considering the co-expression of VEGF-A and VEGFR-1 in MS-K cell line (**Figure 5 & 9**), and the functional activity of VEGFR-1 in MS-K cells (**Figure 10**), a hypothesis was given that VEGF-A facilitated the survival and proliferation of MS-K cells through VEGFR-1 in an autocrine loop.

Proliferation and colony-forming efficiency of *vegfA*-knock down MS-K cells was significantly suppressed under low serum concentration condition, comparing with the control group (**Figure 8**). In the present study, the sequence of dsRNA targeting murine *vegf-A* located in the forth exon of the gene, and it could effectively degrade all the isoforms of VEGF-A protein. While *vegfA*-KD MS-K-GFP cells were cultured in 2% HS medium, there was no difference between VEGF-A quantification in *vegfA*-KD MS-K-GFP culture condition medium and that in normal MS-K or SCR MS-K, suggesting there might be some other factors in serum improve stability of VEGF-A in *vegfA*-KD MS-K-GFP cells to offset the knock down effect. Therefore, it is considered that the rescue of growth and colony formation ability of *vegfA*-knock down MS-K cells is supplied by not only VEGF-A supplemented by serum, but also some factors in serum by improving stability of VEGF-A protein.

In addition, *vegfr-1* knock down MS-K cells also failed to form tumor or form tumor with delayed growth (**Figure 12**), indicating the effect of VEGF-A / VEGFR-1 signal on formation and growth of MS-K tumor. Therefore, it is documented in this study that VEGF-A / VEGFR-1 signal promotes the growth of MS-K cells by autocrine signal loop, and induces and support proliferation of endothelial cells in MS-K tumor by paracrine signal loop (**Figure 23A**). Quantification of VEGF-A produced by *vegf-A* knock down MS-K cells is not able to fit the require for growth of MS-K cells, therefore, if VEGF-A can not be

supplemented from the environment, survival and proliferation of MS-K will be suppressed (**Figure 23B**).

The role of VEGF-A as an essential regulator of angiogenesis in the tumor growth has been well-documented. Also the autocrine action of VEGF on carcinoma cells become the study focus in the world. This study lends evidence to that in spite of the therapy strategies focus on suppressing the tumor angiogenesis, VEGF-A may also be developed to a therapy strategic target to cancer cell self. In addition, better understanding of the mechanisms involved in the downstream signaling of VEGFR-1 will be crucial for elucidation of the effect of VEGF-A and the mechanisms in tumorigenesis.

It was believe that in tumor cell population contains the cancer stem cells (CSCs), which can self-renewal limitlessly and possesses the capacity of differentiation to all types of the tumor cells [35-37]. Moreover, CSCs promote the tumor metastasis [36]. In postnatal life, stem cells derived from different tissues present definitive potency, which can give rise to all cells of the tissue they are derived from, but not cells of other tissues [55]. These characters of adult stem cells, in some aspects, are similar to that of CSCs. However, the self-renewal and differentiation of stem cells are under complex control from both the intrinsic transcription factor network and extrinsic factors in the stem cell niche [56, 57].

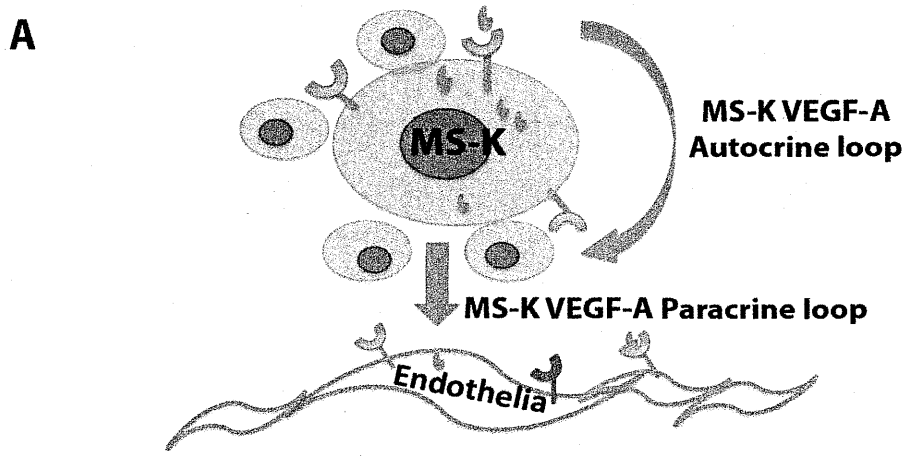

*** MS-K has high expression of *vegf-A*.**

*** VEGF-A produced by MS-K promotes MS-K self-growth by autocrine loop.**

*** VEGF-A produced by MS-K may contribute to proliferation of endothelial cells by paracrine loop *in vivo*.**

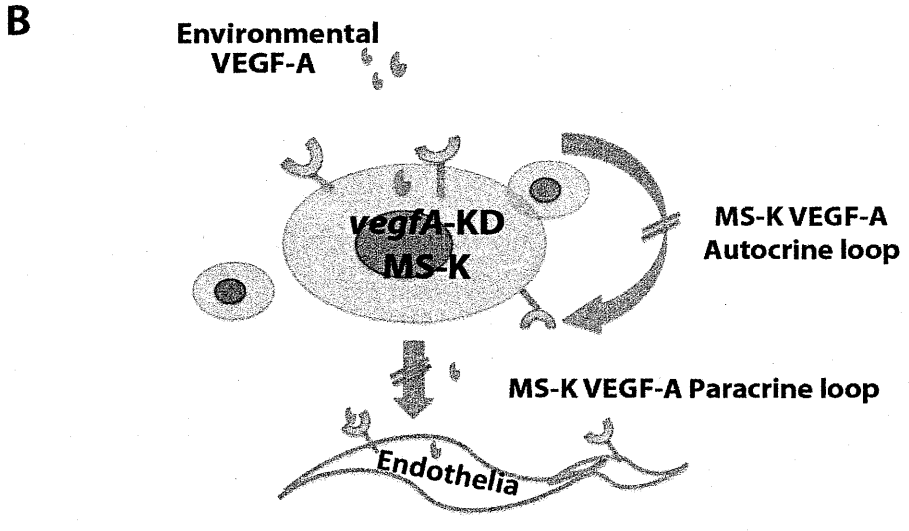

*** Expression of *vegf-A* was suppressed in *vegfA*-KD cells.**

*** Growth of *vegfA-KD* cells become dependent on VEGF-A supplied from the environment.**

Figure 23. Effects of VEGF-A on MS-K tumor formation

VEGF-A produced by MS-K cells promotes growth of MS-K itself by autocrine loop and induces the proliferation of endothelia cells by paracrine loop, which contributes to the growth of MS-K tumor rich in blood vessels and without necrosis.

In this study, *satb*1 was found to have general expression in various kinds of tissues *in vivo*, in contrast, it was only expressed in cells with pluripotency *in vitro* (**Figure 13 & 14**). Recent studies showed that SATB1 controls the balance of self-renewal and differentiation of ES cells and TS cells [24, 25]. The SATB1 also effects the development of brain and epidermis postnatally [27-29]. *satb*2 was found to have an opposite expression profile with *satb*1 in tissues and cell lines. Considering together, it was supposed that *satb*1 may be mainly expressed in primary cells like stem cells or their progenitors in the tissues. *satb1* was reported to be expressed in various types of aggressive cancer cells, and contribute to tumor progression [23, 31-34]. In order to investigate the role of *satb1* in the state regulation of CSC and normal adult stem cells, *satb1* was transiently and stably overexpressed in NIH/3T3 cells. Interestingly, the transcription level of *satb2* was shown to be down-regulated, whereas, expression of *nanog*, was induced in *satb1* overexpressing NIH/3T3 cells. Nanog is known as transcription factor regulating pluripotency of ES cells. It was also documented that overexpression of *nanog* activated other pluripotency genes [58]. However, expression of *oct4* and *sox2* was not detected in *satb1* overexpressing NIH/3T3 cells (**Figure 18**). It was revealed that the P53-P21 pathway served as a barrier in the generation of iPS cells [59]. In this study, up-regulated expression of *p21* and down-regulated expression of *cdk2* were observed in *satb1* overexpressing NIH/3T3 cells, although the expression of *p53* was suppressed in one of the clones (**Figure 17B**). P21, also known as cyclin-dependent kinase inhibitor 1, binds to and inhibits the activity of cyclin-CDK2, and thus functions as a regulator of cell cycle progression at G1 phase. The suppressed growth of both clones of *satb1* overexpressing NIH/3T3 cells in partially confirmed the arrest of cells at G1 phase (**Figure 17A**), suggesting the failed cell reprogramming by only overexpressing *satb1* in fibroblast cell line NIH/3T3.

Study on human ovarian carcinoma showed that *vegf-A* was overexpressed in *satb1* expressing tumor cells [23]. In this work, expression of *vegf-A* in *satb1* overexpressing MS-K cells was not changed (**Figure 19**). *satb1* overexpression endues MS-K cells with enhanced colony formation ability, which made *satb1* overexpressed MS-K cells form colony even just being cultured in alpha-MEM

(**Figure 21**). Moreover, it was confirmed that tumor in *satb1* overexpressing MS-K cells inoculated mice grew faster than the normal MS-K (**Figure 22**). The increased expression of *cdk2* and *bcl2* in *satb1* overexpressing MS-K cells may contribute to the rapid growth of tumor and the enhance colony formation ability (**Figure 20**). Considering together, *satb1* may play different roles in normal cells and tumor cells. Overexpression of *satb1* suppressed the growth of the fibroblast cells NIH/3T3, while for MS-K cells, the overexpression of *satb1* accelerated the growth of tumor, although the improving effect on cell growth was not observed. SATB1, the globe transcription factor, has been reported to play an important role in both stem cells and cancer cells [24, 25, 31-34]. In this study, overexpression of *satb1* in both NIH/3T3 and MS-K induced the expression of *nanog*, which may lend evidence to that *satb1* effect on maintenance of state of not only the normal stem cells but also cancer stem cells [24, 25, 46, 60]. However, the different growth patterns of *satb1* overexpressing NIH/3T3 and *satb1* overexpressing MS-K might suggest the different roles of *satb1* in normal cells and tumor cells. Elucidation of function of SATB1 is expected to make us better understand stem cells and cancer stem cells, and *satb1* overexpressing MS-K is regarded to be a good model for studies on angiogenesis and metastasis.

References:

[1] Masabumi Shibuya. Vascular endothelial growth factor-dependent and -independent regulation of angiogenesis. *BMB report*, 2008, **41**(4): 278-286.

[2] Karamysheva A. F.. Mechanisms of angiogenesis. *Biochemistry* (Moscow). 2008, **73(7)**: 751-762.

[3] He Y.L., Rajantie I., Pajusola K., *et al.* Vascular endothelial cell growth factor receptor 3-mediated activation of lymphatic endothelium is crucial for tumor cell entry and spread via lymphatic vessels. *Cancer Research.* 2005, **65(11)**: 4739-4746.

[4] Roskoski Jr R.. Vascular endothelial growth factor signaling in tumor progression. *Oncology/Hematology.* 2007, **62**: 179–213.

[5] Lohela M., Brya M., Tammelaa T., *et al.* VEGFs and receptors involved in angiogenesis versus lymphangiogenesis. *Current Opinion in Cell Biology.* 2009, **21**:1–12.

[6] Das B., Yeger H., Tsuchida R., *et al.* A hypoxia-driven vascular endothelial growth factor/Flt1 autocrine loop interacts with hypoxia-inducible factor-1A through mitogen-activated protein kinase/extracellular signal-regulated kinase 1/2 pathway in neuroblastoma. *Cancer Research.* 2005, **65(16)**: 7267-7275.

[7] Ferrara N.. Role of vascular endothelial growth factor in regulation of physiological angiogenesis. *Physiol Cell Physiol.* 2001, **280**: 1358–1366.

[8] Heloterä H., Alitalo K.. The VEGF family, the inside story. *Cell.* 2007, **130**: 591-592.

[9] Lee T.H., Seng S., Sekine M., *et al.* Vascular endothelial growth factor mediates intracrine survival in human breast carcinoma cells through internally expressed VEGFR1/FLT1. *Plosmedicine.* 2007, **4(6)**: 1101-1116.

[10] Wartenberg M, Günther J, Hescheler J, *et al.* The embryoid body as a novel in vitro assay system for antiangiogenic agents. *Lab Invest.* 1998, **78(10)**:1301-1314.

[11] Mentlein R., Forstreuter F., Mehdorn H. M., *et al.* Functional significance of vascular ehdothelial growth facator receptor expression on human glioma cells. *Neuro-Oncology.* 2004, **67**: 9–18.

[12] Wang J., Shi Y.Q., Yi J., *et al.* Suppression of growth of pancreatic cancer cell and expression of vascular endothelial growth factor by gene silencing with RNA interference . *Digestive Diseases*. 2008, **9**: 228–237.

[13] Sher I., Adham S. A., Petrik J., *et al.* Autocrine VEGF-A/KDR loop protects epithelial ovarian carcinoma cells from anoikis. *Cancer*. 2009, **124**: 553–561.

[14] Graells J, Vinyals A, Figueras A, *et al.* Overproduction of VEGF concomitantly expressed with its receptors promotes growth and survival of melanoma cells through MAPK and PI3K signaling. *Journal of Investigative Dermatology*. 2004, **123(6)**:1151-61.

[15] Wang S.C., Liu H., Ren L.F., *et al.* Inhibiting colorectal carcinoma growth and metastasis by blocking the expression of VEGF using RNA interference. *Neoplasia*, 2008, **10(4)**: 399-407.

[16] Shibata M-A., Morimoto J., Shibata E., *et al.* Combination therapy with short interfering RNA vectors against VEGF-C and VEGF-A suppresses lymph node and lung metastasis in a mouse immunocopetent mammary cancer model. *Cancer gene rherapy*, 2008, **15**: 776-786.

[17] Ellis L.M., Hicklin D.J.. VEGF-targeted therapy-mechanisms of anti-tumour activity. *Nature review*, 2008, **8**: 579-591.

[18] Raskopf E., Vogt A., Sauerbruch T., *et al.* siRNA targeting VEGF inhibits hepatocellular carcinoma growth and tumor angiogenesis in vivo. *Hepatology*, 2008, **49**: 977–984.

[19] Maziar Shafighi, Radu Olariu, Claudio Brun, *et al.* The role of androgens on hypoxia-inducible factor (HIF)-1 α -induced angiogenesis and on the survival of ischemically challenged skin flaps in a rat model. *Microsurgery*, 2012, on line.

[20] Bond D, Foley E. Autocrine PDGF- VEGF- receptor related (Pvr) pathway activity controls intestinal stem cell proliferation in the adult Drosophila midgut. *Journal of Biology Chemistry*. 2012. on line.

[21] Yang L, Guo X.G., Du C.Q., *et al.* Interleukin-1 Beta Increases Activity of Human Endothelial Progenitor Cells: Involvement of PI3K-Akt Signaling Pathway. *Inflammation*. 2012. on line.

[22] Appukuttan B, McFrland TJ, Stempel A, *et al.* The Related Transcriptional

Enhancer Factor-1 Isoform, TEAD4(216), Can Repress Vascular Endothelial Growth Factor Expression in Mammalian Cells. *PLoS One*. 2012, **7(6)**, on line.

[23] XIANG J.D., ZHOU L.N., LI S.D., *et al*. AT-rich sequence binding protein 1: Contribution to tumor progression and metastasis of human ovarian carcinoma. *Oncology Letters*. 2012. **3**: 865-870.

[24] Fabio Savarese, Amparo Da′ vila, Robert Nechanitzky, and *et al*. Satb1 and Satb2 regulate embryonic stem cell differentiation and Nanog expression. *Genes and Development*. 2009, **23**:2625–2638.

[25] Kazuo Asanoma, Kaiyu Kubota, Damayanti Chakraborty, *et al*. SATB Homeobox Proteins Regulate Trophoblast Stem Cell Renewal and Differentiation. *The Journal of Biological Chemistry*. 2012, **287(3)**: 2257–2268.

[26] Burute M, Gottimukkala K, and Galande S. Chromatin organizer SATB1 is an important determinant of T-cell differentiation. *Immunol Cell Biol*. 2012. On line.

[27] Huang Y, Zhang L, Song N.N., *et al*. Distribution of Satb1 in the central nervous system of adult mice. *Neuroscience Research*. 2011, **71(1)**: 12-21.

[28] Balamotis MA, Tamberg N, Woo YJ, *et al*. Satb1 ablation alters temporal expression of immediate early genes and reduces dendritic spine density during postnatal brain development. *Mol Cell Biol*. 2012, **32(2)**: 333-347.

[29] Fessing MY, Mardaryev AN, Gdula MR, *et al*. p63 regulates Satb1 to control tissue-specific chromatin remodeling during development of the epidermis. *J Cell Biol*. 2011, **194(6)**: 825-839.

[30] Han H.J., Russo Jose, Kohwi Yoshinori, and et al. SATB1 reprogrammes gene expression to breast tumour growth and metastasis. *Nature*, 2008, **452(13)**: 187-195.

[31] Elizabeth Iorns, H. James Hnatyszyn, Pearl Seo, et al. The Role of SATB1 in Breast Cancer Pathogenesis. *JNCI*. 2010. **102(16)**: 1284-1296.

[32] Tu W, Luo M, Wang Z.J.. Upregulation of SATB1 promotes tumor growth and metastasis in liver cancer. *Liver International*. 2012. On line.

[33] Selinger CI, Cooper WA, Al-Sohaily S, et al. Loss of special AT-rich binding

protein 1 expression is a marker of poor survival in lung cancer. *J Thorac Oncol.* 2011, *6(7)*:1179-1189.

[34] McInnes N, Sadlon TJ, Brown CY, et al. FOXP3 and FOXP3-regulated microRNAs suppress SATB1 in breast cancer cells. *Oncogene.* 2012, *31(8)*:1045-54.

[35] Tijana Borovski, Felipe De Sousa E Melo, Louis Vermeulen, et al. Cancer Stem Cell Niche: The Place to Be. *Cancer Research.* 2011, **71**:634-639.

[36] Sampieri K, Fodde R. Cancer stem cells and metastasis. *Semin Cancer Biology*. 2012, **22(3)**:187-193.

[37] Haraguchi N, ishii H, Sakai D, et al. The concept and significance of cancer stem cells. *Nihon Geka Gakkai Zasshi.* 2012, **113(2)**: 204-9.

[38] John E.Dick. Acute myeloid leukemia stem cells. *Annals of The New York Acaaremy of Sciences*. 2005, **1044**: 1-5.

[39] Dominique Bonnet and John E. Dick. Human acute myeloid leukemia is organized as a hierarchy that originates from a primitive hematopoietic cell. *Nature Medicine.* 1997, **3**: 730-737.

[40] Lane SW, Scadden DT, and Gilliland DG. The leukemic stem cell niche: current concepts and therapeutic opportunities. *Blood.* 2009, **114(6)**: 1150-1157.

[41] Fiona M. Watt1, Brigid L. M. Hogan. Out of Eden: Stem Cells and Their Niches. *Science*.2000, **287(5457)**: 1427-1430.

[42] Xi Chen, Han Xu, Ping Yuan, et al. Integration of External Signaling Pathways with the Core Transcriptional Network in Embryonic Stem Cells. *Cell.* 2008. **133**: 1106–1117.

[43] Kang YJ, Shin JW, Yoon JH, et al. Inhibition of erythropoiesis by Smad6 in human cord blood hematopoietic stem cells. *Biochem Biophys Res Commun.* 2012. On line.

[44] Tashiro K, Kawabata K, Omori M, et al. Promotion of hematopoietic differentiation from mouse induced pluripotent stem cells by transient HoxB4 transduction. *Stem Cell Research.* 2012, **8(2)**:300-11.

[45] Corey Heffernan, Huseyin Sumer, Luis F. Malaver-Ortega, et al. Temporal Requirements of cMyc Protein for Reprogramming Mouse Fibroblasts. *Stem*

Cells Int. 2012, on line.

[46] Collene R. Jeter, Mark Badeaux, Grace Choy, et al. Functional Evidence that the Self-Renewal Gene NANOG Regulates Human Tumor Development. *Stem Cells*. 2009, **27(5)**: 993–1005.

[47] Uchino K, Hirano G, Hirahashi M, et al. Human Nanog pseudogene8 promotes the proliferation of gastrointestinal cancer cells. *Exp Cell Res*. 2012, **318(15)**:1799-807.

[48] Shirata K., Suzuki T., Yanaihara N., *et al*. Establishment of a sarcoma cell line, MS-K, expressing Ki-ras proto-oncogene product from mouse bone marrow stromal cells. *Biomed and Pharmacother*. 1991, **45**: 1-8.

[49] Itoh, K., Tezuka, H., Sakoda, H., et al. Reproducible establishment of hemopoietic supportive stromal cell lines from murine bone marrow. *Exp. Hematol*. 1989, **17**: 145–153.

[50] Polzikov M, Magoulas C, Zatsepina O. The nucleolar protein SURF-6 is essential for viability in mouse NIH/3T3 cells. *Mol Biol Rep*. **34(3)**:155-60.

[51] Luka Milas, Evan M. Hersh, and Nancy Hunter. Therapy of Artificial and Spontaneous metastases of Murine Tumors with Maleic Anhydride-Divinyl Ether-21. *Cancer Research*. 1981, **41**, 2378-2385.

[52] Kaori Imadome, Mayumi Iwakawa, Kazunori Nojiri, et al. Upregulation of stress-response genes with cell cycle arrest induced by carbon ion irradiation in multiple murine tumors models. *Cancer Biology & Therapy*. 2008, **7(2)**: 208-217.

[53] Toda, K., Tsujioka, K., Maruguchi, Y., et al. Establishment and characterization of a tumorigenic murine vascular endothelial cell line (F-2). *Cancer Res*. 1990, **50**: 5526–5530.

[54] Takahashi K, Yamanaka S. Induction of pluripotent stem cells from mouse embryonic and adult fibroblast cultures by defined factors. *Cell*. 2006, **126(4)**: 663-76.

[55] Abhishek Sohni, Catherine M. Verfaillie. Multipotent adult progenitor cells. *Best Practice and Research Clinical Haematology*. 2011, **24(1)**: 3-11.

[56] Paolo Bianco. Bone and the hematopoietic niche: a tale of two stem cells. *Blood*, 2011, **117(20)**: 5281-5288.

[57] Fiona M. Watt1, Brigid L. M. Hogan. Out of Eden: Stem Cells and Their Niches. *Science*. 2000, **287(5457)**: 1427-1430.

[58] Picanço-Castro V, Russo-Carbolante E, Covas DT. Forced expression of nanog in human bone marrow-derived endothelial cells activates other six pluripotent genes. *Cell Reprogram*. 2012, **14(3)**:187-192.

[59] Hyenjong Hong, Kazutoshi Takahashi, Tomoko Ichisaka, et al. Suppression of induced pluripotent stem cell generation by the p53–p21 pathway. *Nature*. 2009, **460**: 1132-1136.

[60] Manish V. Baisa, Zabrina M. Shabina, Megan Younga, *et al*. Role of Nanog in the maintenance of marrow stromal stem cells during post natal bone regeneration. *Biochemical and Biophysical Research Communications*. 2012, **417(6)**: 211–216.

Acknowledgements

First and foremost, I would like to show my deepest gratitude to my supervisor, Dr. Sugimoto, a respectable, responsible and resourceful scholar, who has provided me with valuable guidance in every stage of the writing of this thesis. Without his strong support and patient instruction, this thesis could not have been the present form.

I shall extend my thanks to Dr. Touma and the members in Sugimoto Lab. for all their kindness and help.

I would also like to thank all my professors who have helped me to develop the fundamental and essential academic competence.

Last but not least, I'd like to thank my parents and my family for their encouragement and support.